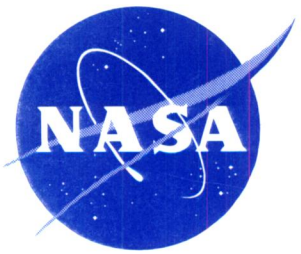

NASA Technical Paper 3488

NASA-TP-3488 19940033066

Aerodynamic Characteristics of the National Launch System (NLS) 1½ Stage Launch Vehicle

A.M. Springer and D.C. Pokora

May 1994

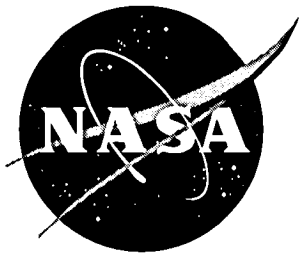

NASA Technical Paper 3488

Aerodynamic Characteristics of the National Launch System (NLS) 1½ Stage Launch Vehicle

A.M. Springer and D.C. Pokora
Marshall Space Flight Center • Huntsville, Alabama

National Aeronautics and Space Administration
Marshall Space Flight Center • Huntsville, Alabama 35812

May 1994

ACKNOWLEDGMENT

The authors would like to thank the wind tunnel test team at MSFC for their help in making these wind tunnel tests a success: H. Brewster, H. Gwin, S. Espey, A. Frost, C. Dill, T. Schmitt, S. Stewart, J. Heaman, and M. Niedermeyer.

TABLE OF CONTENTS

LIST OF ILLUSTRATIONS

LIST OF ILLUSTRATIONS (Continued)

LIST OF ILLUSTRATIONS (Concluded)

NOMENCLATURE

Symbol	Description
$A_{b_{CS}}$	core projected base area, 646.2 ft^2 (full scale) (z-y plane)
$A_{b_{ASRB}}$	ASRB base area, 236.11 ft^2 (full scale)
alpha, α	angle-of-attack, degrees
A_{ref}	reference area, 593.96 ft^2 (full scale)
beta, β	angle-of-sideslip, degrees
C_A	axial force coefficient
C_{A_o}	forebody axial force coefficient at zero angle-of-attack/angle-of-sideslip
C_l	rolling moment coefficient
$C_{l\beta}$	rolling moment coefficient slope w.r.t. angle-of-sideslip
C_M	pitching moment coefficient
$C_{M\alpha}$	pitching moment coefficient slope w.r.t. angle-of-attack
C_N	normal force coefficient
$C_{N\alpha}$	normal force coefficient slope w.r.t. angle-of-attack
C_n	yawing moment coefficients
$C_{n\beta}$	yawing moment coefficients slope w.r.t. angle-of-sideslip
C_P	pressure coefficient for tap $P(n)$
C_{P_b}	base pressure coefficient
C_Y	side force coefficient
$C_{Y\beta}$	side force coefficient slope w.r.t. angle-of-sideslip
$\frac{dC_A}{d(X/D)}$	axial force coefficient per caliber

$\frac{dC_{M\alpha}}{d(X/D)}$	pitching moment coefficient slope w.r.t. angle-of-attack per caliber
$\frac{dC_{M\alpha}}{d(X/D)}$	normal force coefficient slope w.r.t. angle-of-attack per caliber
D_{ref}	reference diameter, 27.5 ft (full scale)
F_{A_T}	total axial force
$F_{AB_{\text{ref}}}$	power-on base axial force, aerodynamic reference trajectory
L_{ref}	reference length, 27.5 ft (full scale)
MACH	Mach number
MRP (X_T, Y_T, Z_T)	moment reference point (4385.5, 0, 0)
P	measured local static pressure
P_{inf}	free stream pressure
P_b	element base pressure
Q	dynamic pressure
X_{CP}	model center of pressure from MRP, inches
X	vehicle axial location (full scale)
X/D	dimensionless distance from vehicle nose ($D = D_{\text{ref}}$)
X/L	dimensionless distance from vehicle nose ($L = L_{\text{ref}}$)

TECHNICAL PAPER

AERODYNAMIC CHARACTERISTICS OF THE NATIONAL LAUNCH SYSTEM (NLS) 1½ STAGE LAUNCH VEHICLE

I. INTRODUCTION

The National Launch System (NLS) is a joint National Aeronautics and Space Administration/ Department of Defense (NASA/DOD) program to develop a family of launch vehicles that have common elements. Initially this family consisted of a heavy lift launch vehicle (HLLV) configuration designed to launch 100 to 150 klb payloads and a 1½ stage vehicle to launch 50 klb payloads (reference 1). This document will deal with the aerodynamic characteristics of the 1½ stage configuration.

To support the detailed configuration definition, two wind tunnel tests, TWT 733 and TWT 734, were run in the Marshall Space Flight Center's (MSFC's) 14×14-Inch Trisonic Wind Tunnel (TWT) facility to determine the effect of configuration variations on vehicle aerodynamics and a reference aerodynamic database. TWT 733 was a static stability test that resulted in forces and moments for the 1½ stage configuration. Variations in engine shroud design and the option of feedlines were studied. The second wind tunnel test, TWT 734, was a pressure test. TWT 734 resulted in the pressure distributions for various conditions over the vehicle with and without feedlines. This data is to be utilized consistently with the force and moment results from TWT 733, thus assuring consistent data bases for trajectory, control, and loads systems studies. All test models are 0.004 scale.

The 1½ stage vehicle consists of a cylindrical cargo element (the current Titan IV shroud) with a biconic nose cone and a 17°12' interstage mounted on top of a modified Space Transportation System (STS) external tank (ET). Modifications to the ET consist of stretching the hydrogen tank and liquid oxygen (lox) tank to accommodate the liquid propulsion system added to its base. This propulsion system consists of six STME engines with four engine shrouds. Figure 1 shows the 1½ stage launch vehicle configuration static stability model in the MSFC 14×14-Inch TWT. Figure 2 depicts the NLS 1½ stage vehicle geometry.

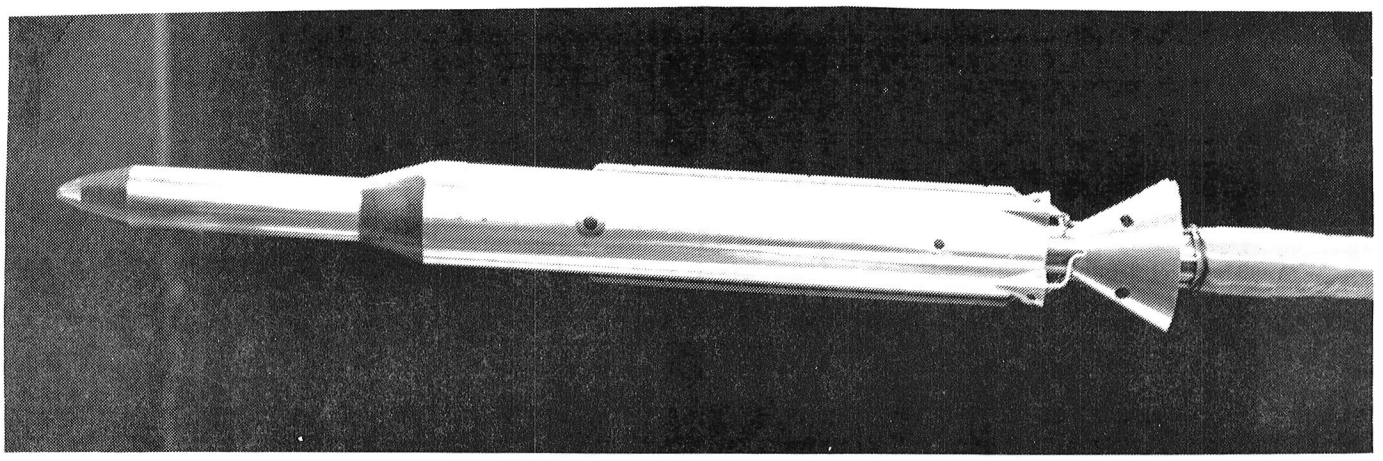

Figure 1. NLS 1½ stage vehicle static stability model mounted in the MSFC 14×14-Inch TWT.

AREF=593.96 sq. ft.
DREF=27. 5 ft.

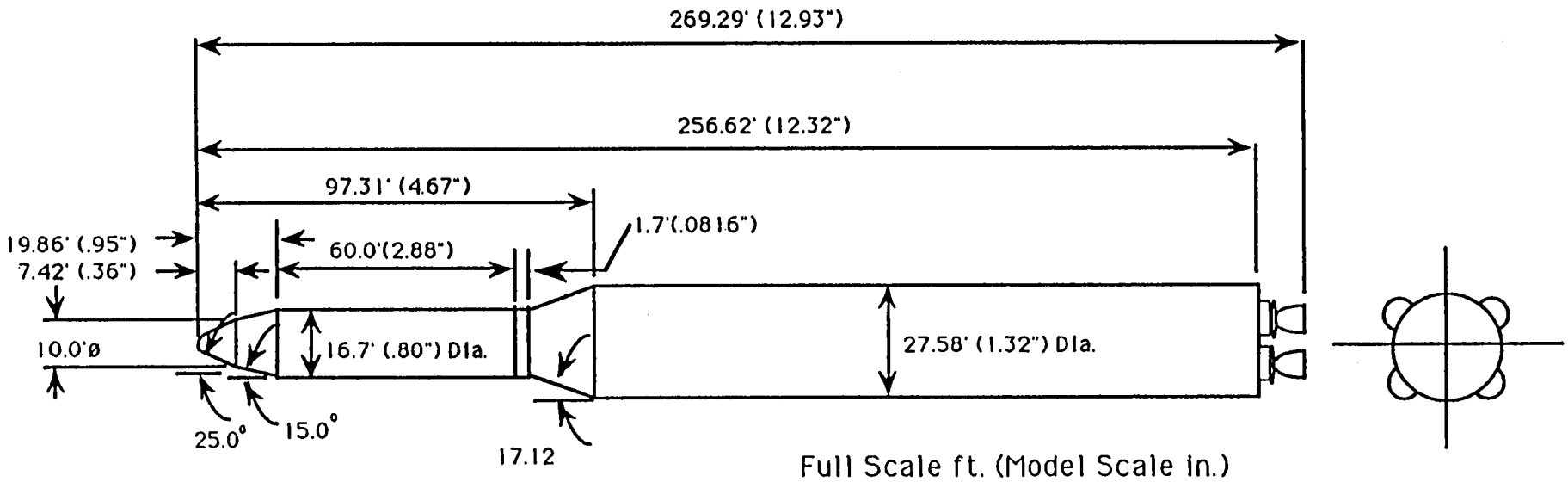

Figure 2. NLS 1½ stage vehicle geometry.

II. TEST FACILITY DESCRIPTION

The MSFC 14×14-Inch TWT is an intermittent blowdown tunnel which operates by high pressure air flowing from storage to either vacuum or atmosphere conditions. The transonic test section provides a Mach number range from 0.2 to 2.0. Mach numbers between 0.2 and 0.9 are obtained by using a controllable diffuser. The Mach range from 0.95 and 1.3 is achieved through the use of plenum suction and perforated walls. Each Mach number above 1.3 requires a specific set of two-dimensional contoured nozzle blocks. A solid wall supersonic test section provides the entire range from 2.74 to 5.0 with one set of automatically actuated contour blocks. Air is supplied to a 6,000 ft^3 storage tank at approximately –40 °F dewpoint and 425 lb/in^2 gauge. The compressor is a three-stage reciprocating unit driven by a 1,500 hp motor. The tunnel flow is established and controlled with a servo-actuated gate valve. The controlled air flows through the valve diffuser into the stilling chamber and heat exchanger where the air temperature can be controlled from ambient to approximately 180 °F. The air then passes through the test section, which contains the nozzle blocks and test region. Downstream of the test section is a hydraulically controlled pitch sector that provides the capability of testing up to 20 angles-of-attack from –10 to +10 degrees during each run. Sting offsets are available for obtaining various maximum angles-of-attack up to 90°. The diffuser section has movable floor and ceiling panels, which are the primary means of controlling the subsonic Mach numbers and permit more efficient running supersonically. Tunnel flow is exhausted through an acoustically damped tower to atmosphere or into the vacuum field of 42,000 ft^3. The vacuum tanks are evacuated by vacuum pumps driven by a total of 500 hp.

The data acquisition system (DAS) is a Hewlett-Packard (HP) 349A controller with a HP 3456A digitizer. The unit is equipped with various control modules for facility system control, angle-of-attack readout, Scanivalve control, etc. Currently, the system is configured to 40 low-level strain gauge, thermocouple, or pressure channels per second, with a 2- or 3-s recycle time to change angle-of-attack and allow for settling. Low pass filters are available for all channels and are routinely used on strain gauge balance channels. System control and data reduction are by a HP 200-series computer with a 1-Mbyte memory. Data is reduced after each run, and tabulated data is available in about 20 s using a HP laser jet printer. All data are stored on disk for subsequent transfer to another computer for further analysis or data base construction.

On-line data are reduced to coefficient form by a solid-state data acquisition and computing system. Hard copies of tabulated data and preliminary plots are provided a few minutes after each run. More detailed information on the 14×14-Inch TWT is contained in reference 2.

III. MODEL DESCRIPTIONS

The 1½ stage vehicle models consist of a cylindrical payload section 2.88 inches in length, 0.800 inches in diameter with a biconic nose cone (15°/25°). The interstage section (0.838 inches in length) connects the payload section to an ET section that has been modified to include an addition 5 ft, full scale, in length (ET section, including the propulsion module, is 7.647 inches in length and 1.324 inches in diameter). The reference configuration engine shrouds are made to be removable and are 0.692 inches in length and have a 0.252-inch radius. A 1½ stage optimum shroud design, 0.882 inches in length and 0.662 inches in radius, was also tested. The HLLV optimum shroud design, 0.682 inches in length and 0.662 inches in radius, was also tested on the 1.5 stage configuration. The model utilizes removable feedlines which are 5.28 inches in length with side extensions 110° from the centerline blending into the engine shrouds. Figure 3 depicts the three engine shroud configurations tested for the 1½ stage configuration.

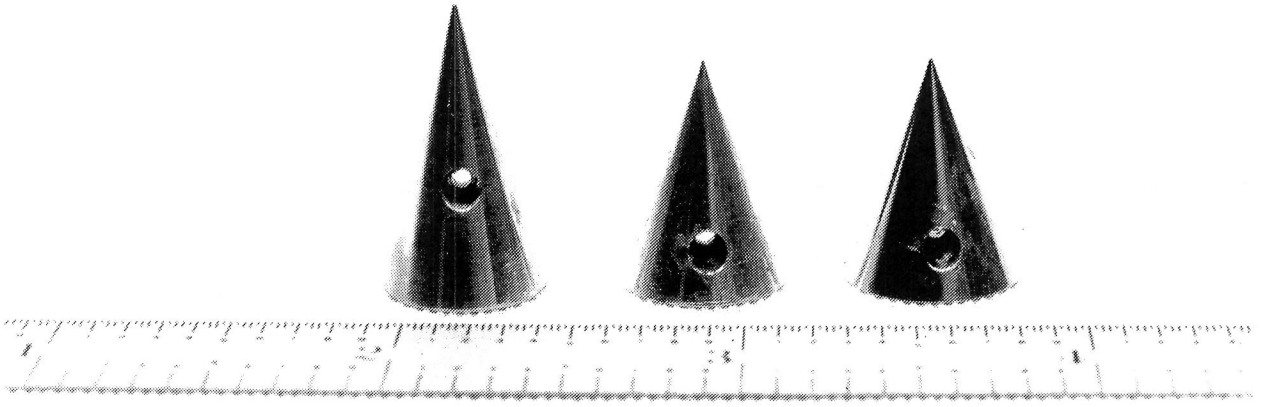

Figure 3. Engine shroud configurations tested.

Due to the complexity of fabrication/assembly/cost, existing stock materials were utilized for the lox feedlines. Therefore, the dimensions for the feedlines do not correspond exactly to the reference configuration feedline dimensions. The effects are considered to be small on the total vehicle aerodynamics. For plume simulation, a solid plume and a flat plate were utilized to match analytically determined base pressure values. Model dimensions are identical for the static stability and pressure models. The solid plume simulator can be seen in figure 1, the frustum mounted to the sting aft of the base of the vehicle.

The 1½ stage configuration pressure model was instrumented with 233 pressure taps located at various stations shown in figure 4. Ports were nominally placed at 22.5° increments in quadrant I and III. This setup allowed for a full set of pressure data to be obtained with the fewest taps. The locations of ports at an example station is shown in figure 5. A closeup of the nose region of the pressure model is shown in figure 6. Two taps were found to be bad and were deleted from the data. These taps were not seen to be detrimental to the test, so the test proceeded without them.

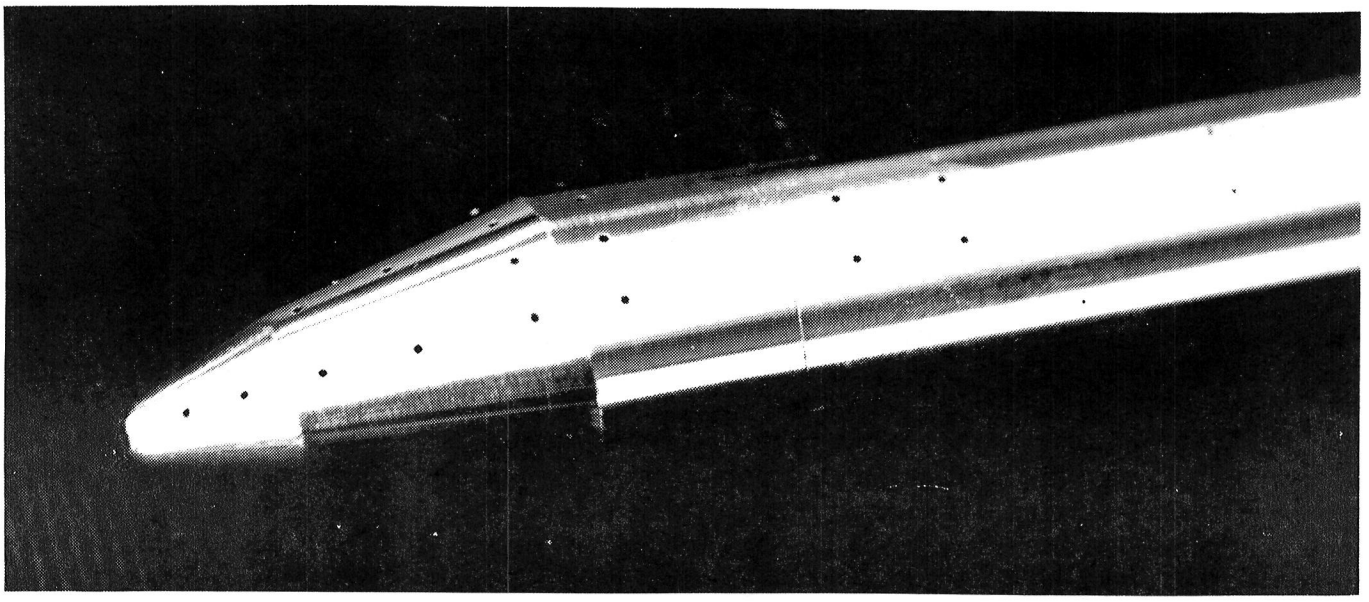

Figure 4. Closeup of NLS 1½ stage pressure model.

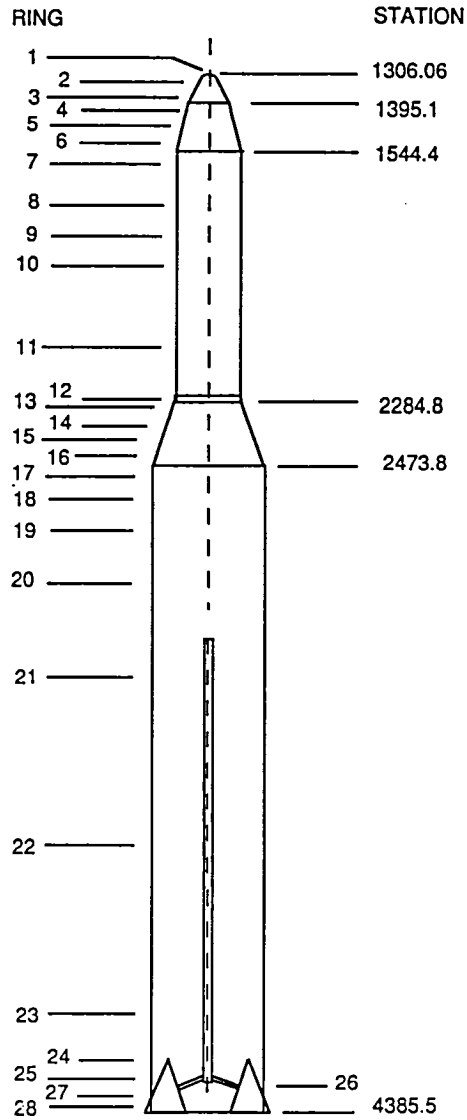

Figure 5. Example pressure tap phi locations at a given station.

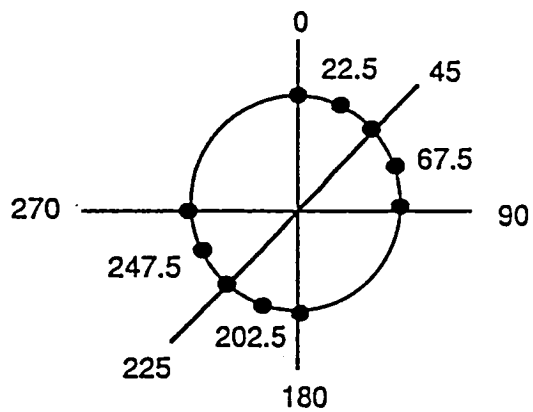

Figure 6. Closeup of ring location of pressure tap stations.

IV. TEST PROCEDURE

For both tests, testing was done over a Mach range of 0.6 to 4.96. The angle-of-attack and angle-of-sideslip ranges for each run were –8° to +8° for the static stability test and –4° to +8° for the pressure test, both in 2° increments.

The test schedule involved testing each configuration for a predetermined, standard set of 13 Mach numbers.

The pressure test required two sets of pressure tap data to obtain a full set of vehicle pressure coefficients. This is due to the limited number of pressure transducers in the DAS. The tap hookups are defined as hookup/tapset A and hookup/tapset B. Setup A is the forward part of the vehicle past the frustum, ring 1 to 18, including all the taps at phi angles of 0°, 90°, 180°, and 270° along the whole vehicle. Setup B is

the aft part of the vehicle ring, 14 to 28, including all the taps at phi angles of 0°, 90°, 180°, and 270° along the whole vehicle.

A series of shadowgraphs were run during and following the static stability test. A representative shadowgraph is shown in figure 7. The accompanying shadowgraph study of the NLS 1½ stage configuration is presented in reference 3.

A. Solid Plume Simulation

Plume studies were done for the 1½ stage reference configuration for the static stability and pressure tests over the entire Mach range. The plume locations for each test were measured from the base of the vehicle. A study was also done during the pressure test to determine the base pressures for which plume-induced flow separation occurred on the vehicle and how far forward the separation occurred. The results from this study are presented in reference 4. The simulated plume for the 1½ stage vehicle is shown in figure 1. The general study used the solid plume alone up to Mach 1.96 and added the flat plate at the higher Mach numbers. The separation study used the plume with the flat plate reversed, so the flat plate was toward the vehicle, allowing the highest pressure to be obtained.

A more detailed description of the two wind tunnel tests, TWT 733, the static stability test, and TWT 734, the pressure test, can be found in references 5 and 6, respectfully.

V. INSTRUMENTATION AND DATA REDUCTION

A. Static Stability Measurements

The six-component balance on which the model was mounted measured total mated vehicle forces and moments. Six-component force and moment coefficients were computed from the main balance about its axis system and then transferred to the moment reference point shown in figure 8. Forebody coefficients were calculated using the element base-pressure results. Angles-of-attack and angles-of-sideslip were calculated from the sector reading, taking into account the sting and balance deflections determined using pretest calibrations.

B. Pressure Measurements

Model base pressures were measured using external tubes placed next to the base of each element, as shown in figure 9, and are sampled by transducers mounted outside the test section as are all other measurements. The same position/proximity for both tests were used.

The pressure model used 0.032-inch tubing for the pressure taps, converted to 0.064 inch for the DAS. All pressure data were reduced to coefficient form as follows:

$$C_P(n) = \frac{P(n) - P_{\text{inf}}}{Q_{\text{inf}}};\ n = 1 -> 233.$$

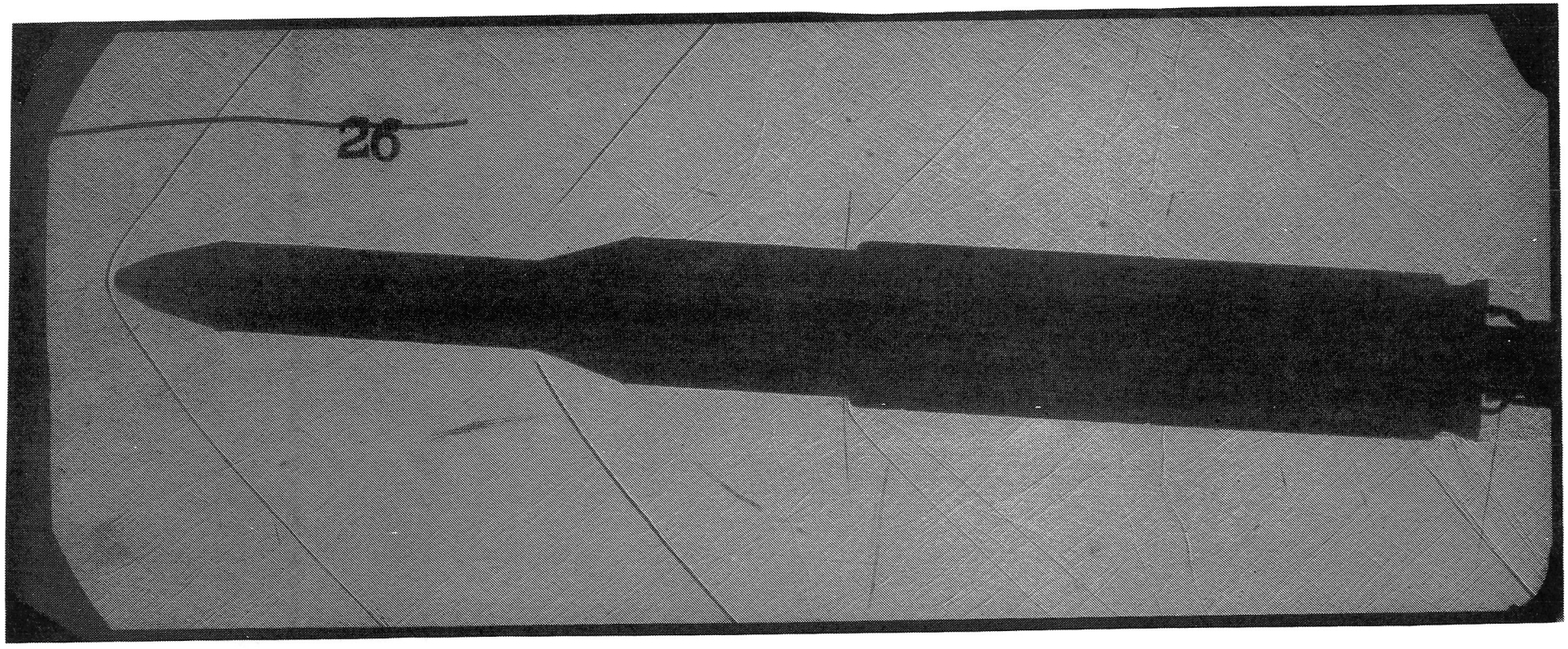

Figure 7. Shadowgraph of NLS 1½ stage configuration at Mach 1.46; $\alpha = 4$, $\beta = 0$.

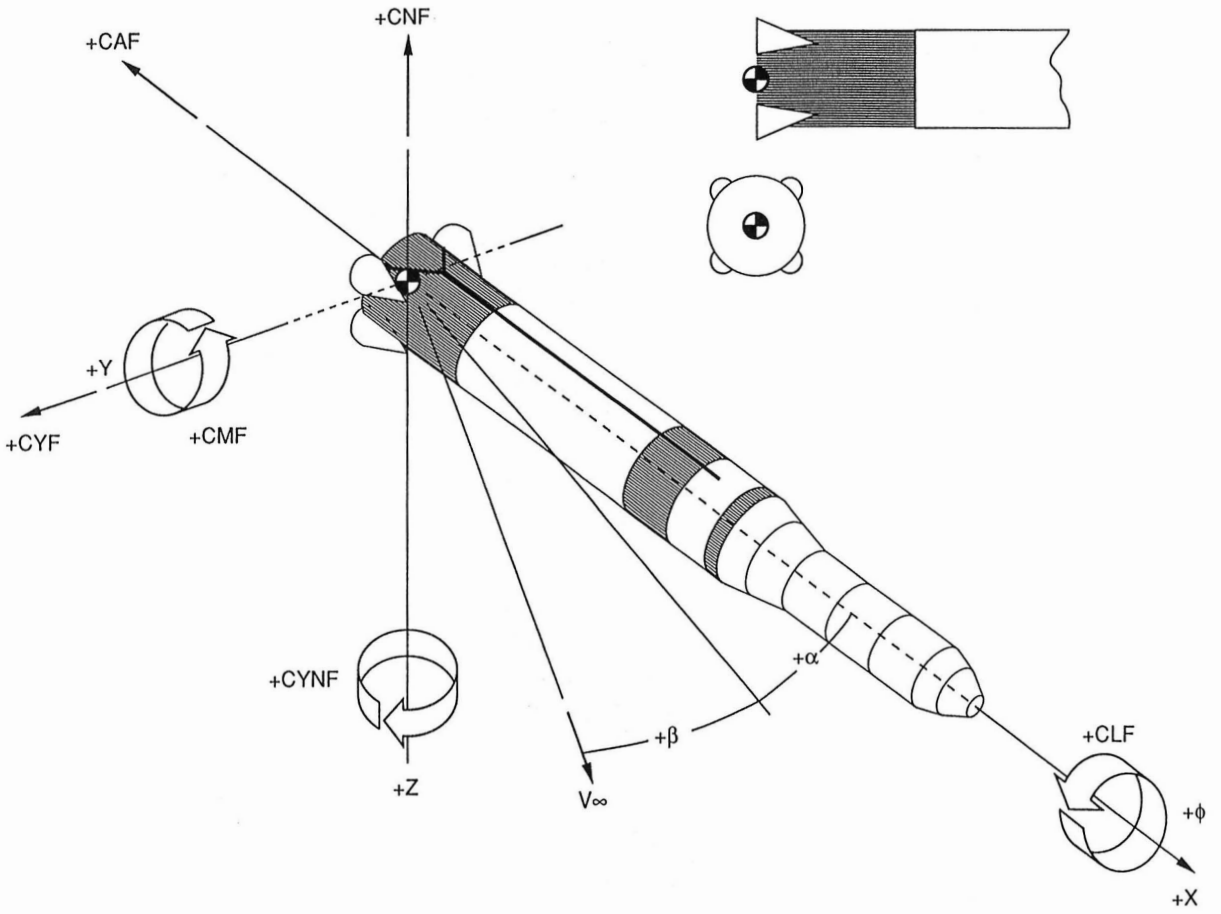

Figure 8. Aerodynamic axis system.

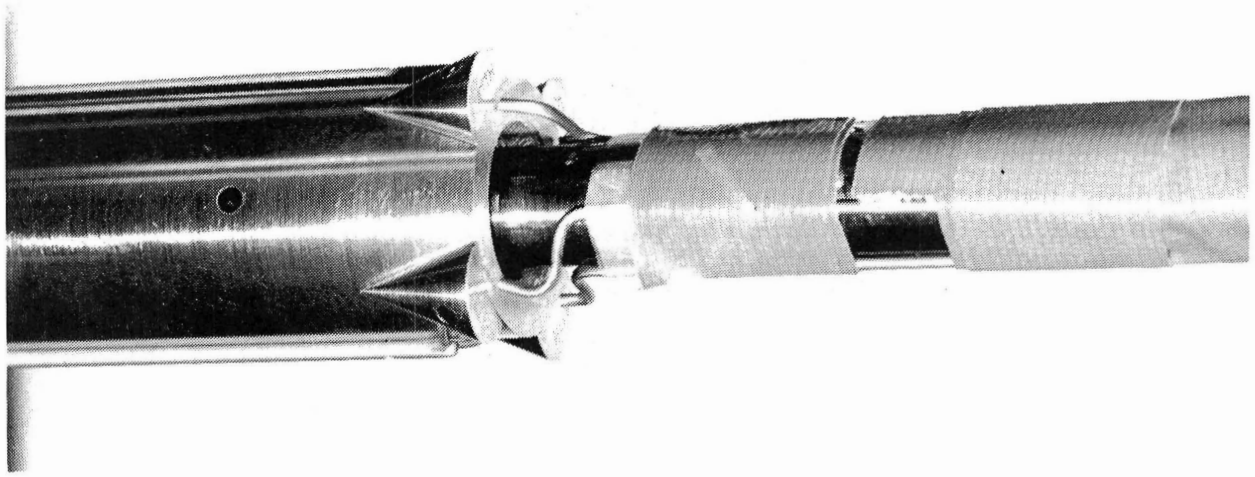

Figure 9. Base pressure locations.

VI. RESULTS

A. Static Stability Test

The 1½ stage aerodynamic data base consists of vehicle data including plume effects. This data was determined as a result of the test performed in the MSFC 14×14-Inch TWT (see ref. (5)). The data (forces and moments) are to be applied at the moment reference point (MRP). Figure 8 shows the aerodynamic axis system for the data base. The MRP for which the data base originates is shown to be located at the base of the vehicle (see fig. 8).

The data base contains the force and moment coefficients, linearized as slopes of the longitudinal data with respect to alpha and of the lateral data with respect to beta. The coefficients of the longitudinal data are normal force, C_N; pitching moment, C_M; and axial force, C_A. The coefficients of the lateral data are side force, C_Y; yawing moment, C_n; and rolling moment, C_l. C_l for this configuration is essentially zero, due to the symmetry of the vehicle. Figure 10 is a graphical representation of the linearized data. Figures 11 through 15 show the aerodynamic coefficients verses Mach for the 1½ stage configuration.

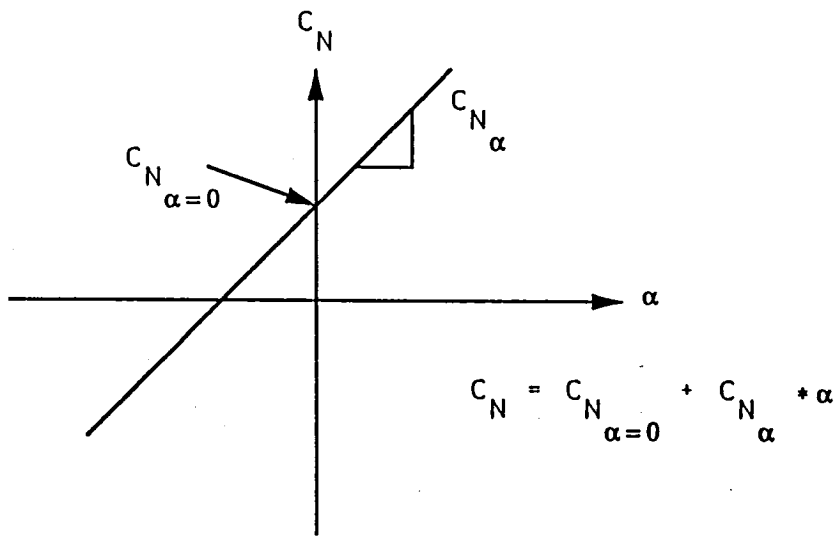

Figure 10. Linearized aerodynamics.

If a force/moment is desired, the aerodynamic coefficients can be converted using the following equations:

$$C_N = C_{N\alpha} * \alpha$$
$$C_Y = C_{Y\beta} * \beta$$
$$C_M = C_{M\alpha} * \alpha$$
$$C_l = C_{l\beta} * \beta$$

Force = Coeff. (C_N, C_A, C_Y) * Q * A_{ref}
Moment = Coeff. (C_M, C_n, C_l) * Q * A_{ref} * D_{ref}.

Note: These equations are for a symmetric vehicle, i.e., all coefficients are zero at $\alpha/\beta = 0$.

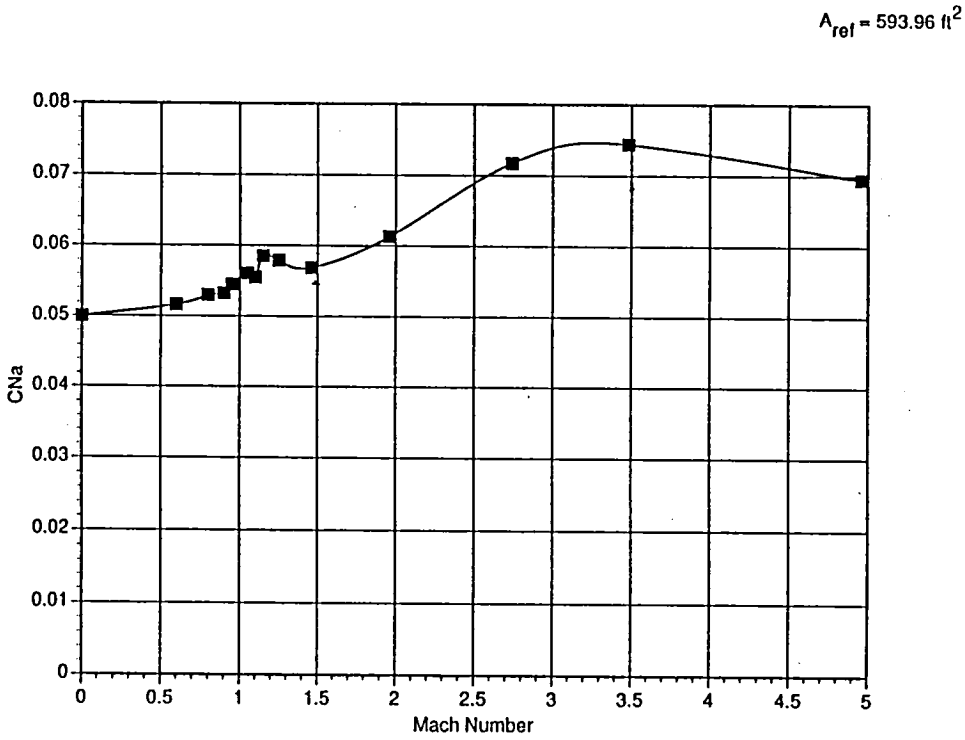

Figure 11. $C_{N\alpha}$ versus Mach.

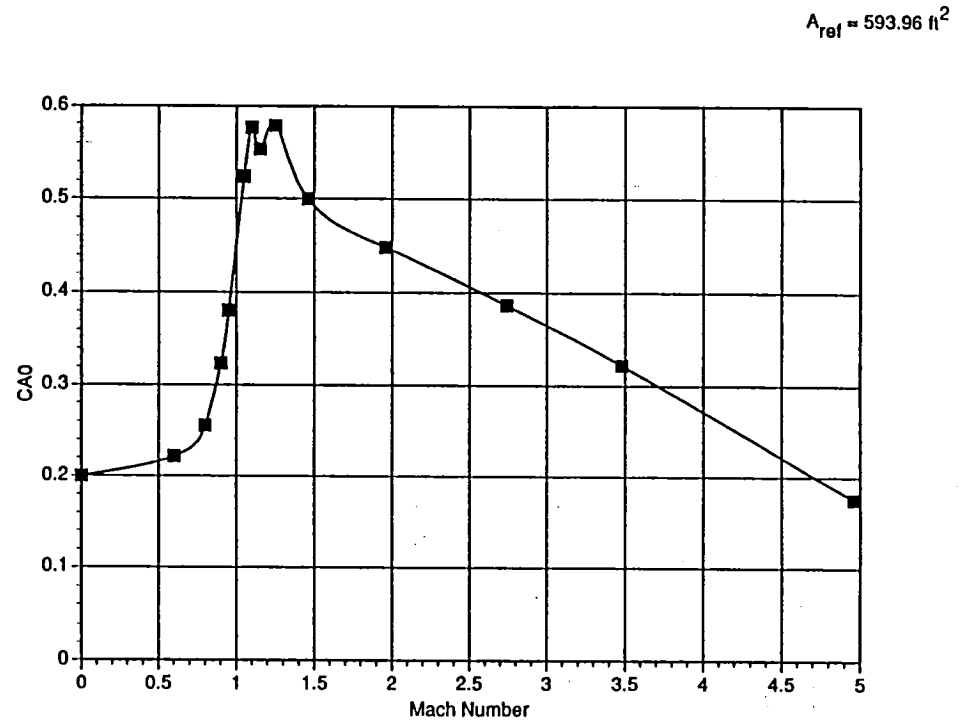

Figure 12. C_{A0} versus Mach.

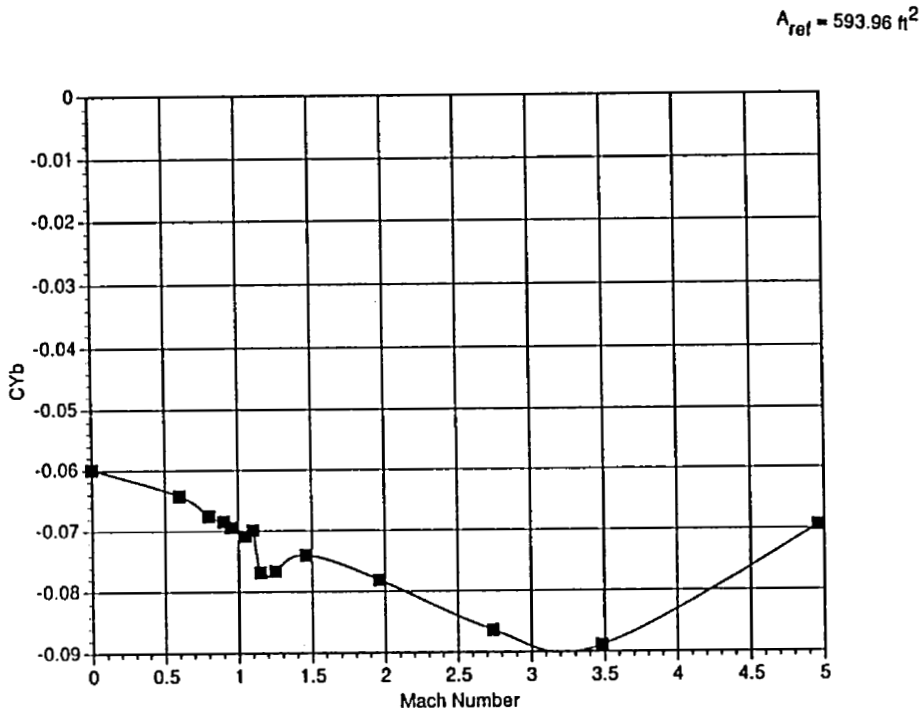

Figure 13. $C_{Y\beta}$ versus Mach.

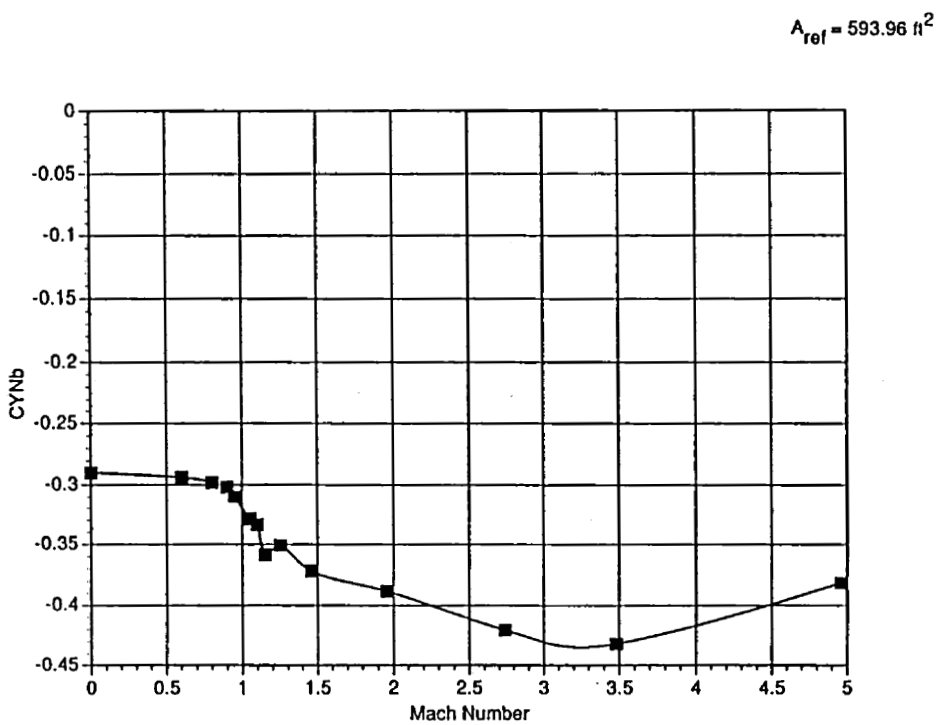

Figure 14. $C_{l\beta}$ versus Mach.

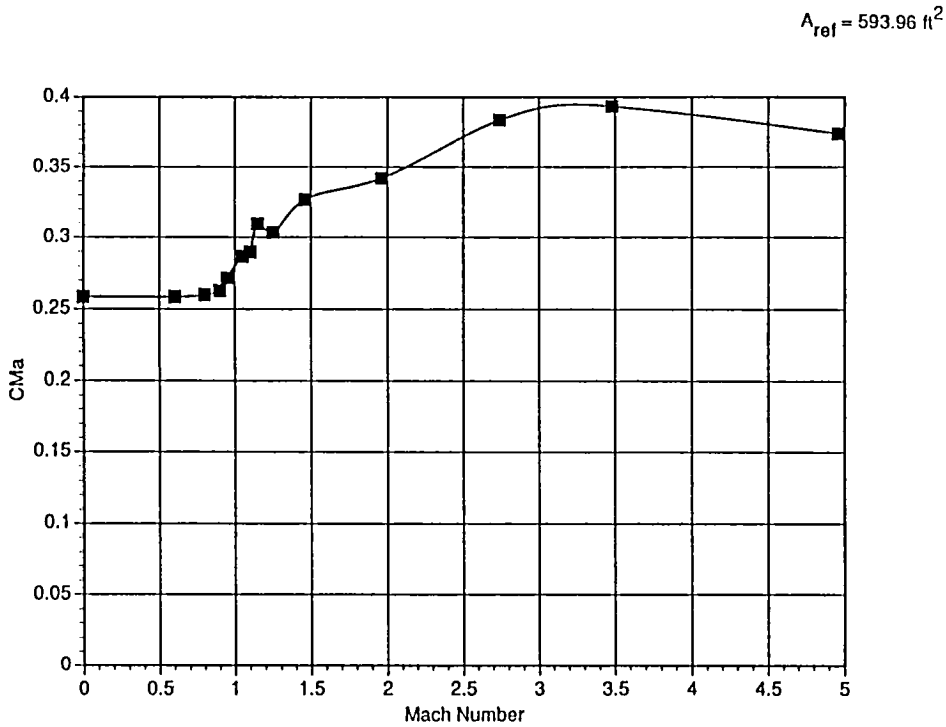

Figure 15. $C_{M\alpha}$ versus Mach.

Power-on base axial force data, F_{AB} (klb) as a function of altitude (kft), dynamic pressure, Q, thrust (lb), and Mach was determined. This base force is derived from the 1½ stage reference ascent flight trajectory. Base axial force, F_{AB} verses altitude is shown in figure 16. Figure 17 shows the reference dynamic pressure versus altitude.

The total axial force is determined by the sum of the base axial force and the forebody axial force as shown below:

$$F_{A_T} = C_{A_o} * Q * A_{\text{ref}} + F_{AB_{\text{ref}}}$$

The resulting aerodynamic characteristics from the static stability test are presented in tabular format in appendix A.

B. Pressure Test

The pressure test resulted in 231 individual pressure coefficients over the body of the vehicle for the range of Mach numbers and angles-of-attack tested. Extraneous points were removed from the data. The resulting data sets were interpreted to even angle-of-attack. This data was then mirrored to cover the surface of the vehicle. At points where data was lacking, due to the number of taps or a bad data point, the surrounding data was used to spline the missing data into the data set.

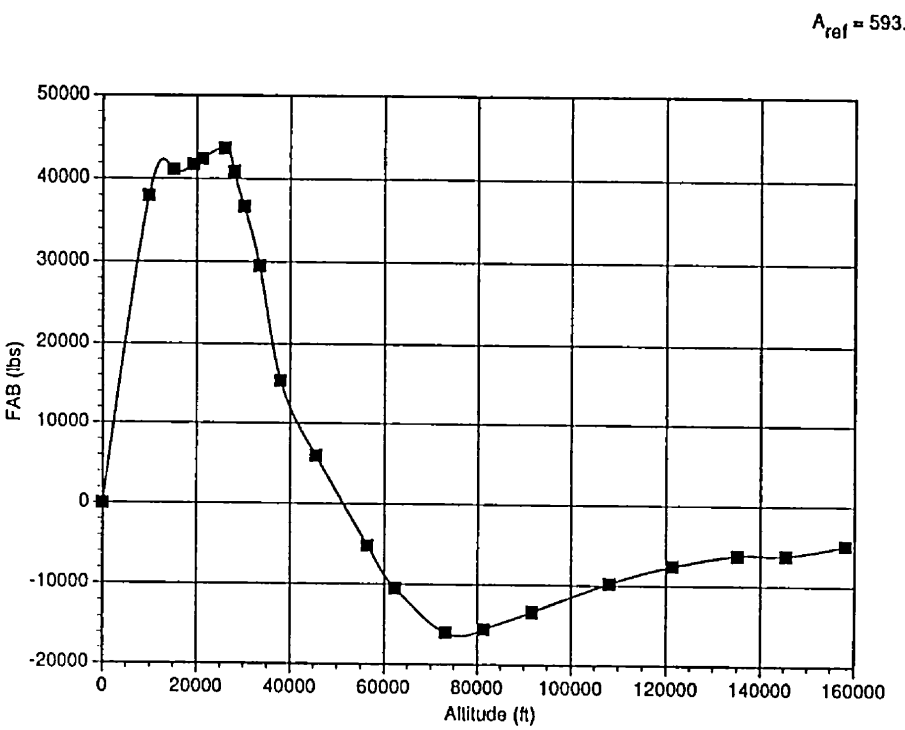

Figure 16. Base axial force (F_{AB}) versus altitude.

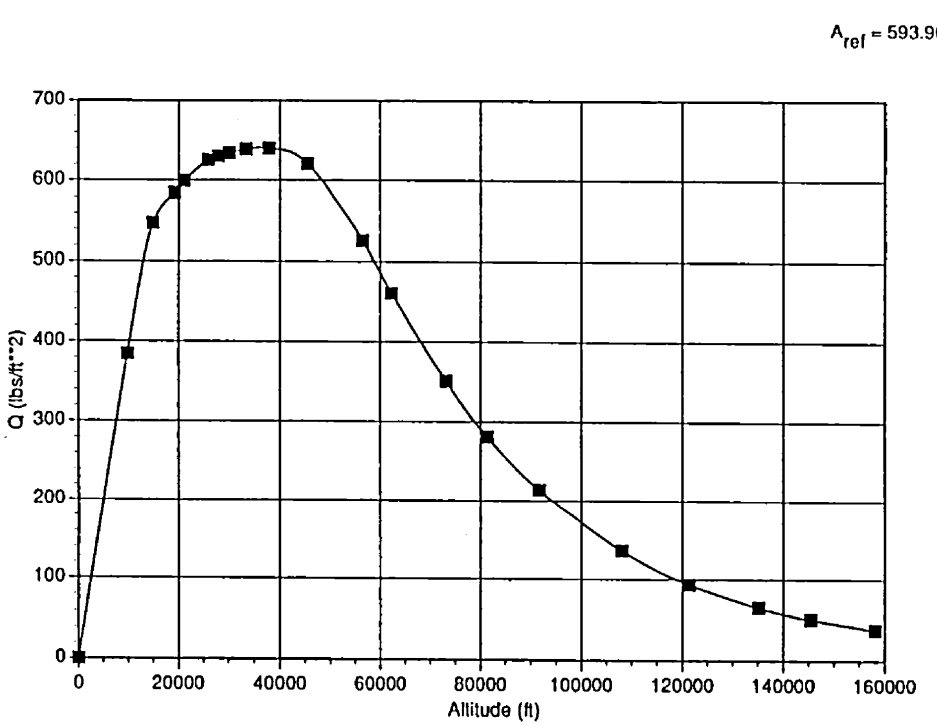

Figure 17. Dynamic pressure (Q) versus altitude.

C. Distributed Loads

Normal force coefficient slope with respect to angle-of-attack, $\frac{dC_{N\alpha}}{d(X/D)}$, pitching moment coefficient slope with respect to angle-of-attack, $\frac{dC_{M\alpha}}{d(X/D)}$, and axial force coefficient, $\frac{dC_A}{d(X/D)}$, distributions have been generated for the 1½ stage vehicle configuration of the NLS. These distributed loads were determined over the transonic Mach range.

A normal force coefficient slope distribution and pitching moment coefficient slope distribution were created using pressure data from reference (6) integrated and matched to data from reference (5). This ensures consistency between the aerodynamic data used for performance, trajectory, control, and loads studies. The running load distributions were balanced to the data in reference (5) to nominally within 10 percent (5 percent normal force and 10 percent pitching moment). No criteria has yet been established requiring a closer balance between forces/moment data and load distributions. The balancing and integration of the data was done using the following MacIntosh programs: MCP—pressure data integration and initial distributed loads, Kaleidagraph—integration of distributed loads, Excel—data analysis, and DeltaGraph Professional—plotting of data. Figure 8 shows the aerodynamic axis system for the 1½ stage vehicle and defines the reference dimensions utilized in the data base.

The axial force coefficient distribution was also created using the preceding methods. The axial force coefficient running load distributions were balanced to the data in reference (5) to within 5 percent.

The preceding data sets can be used to determine the local normal force distribution, local pitching moment distribution, local axial force distribution, and component loading on the vehicle. The force is determined by the following:

$$\text{Local normal force} = \frac{dC_{N\alpha}}{d(X/D)} * Q * A_{\text{ref}} * \alpha$$

$$\text{Local axial force} = \frac{dC_A}{d(X/D)} * Q * A_{\text{ref}}.$$

The loading on a component of the vehicle (e.g., interstage) is determined by integration of the distribution over the component

$$\frac{dC_N}{d(X/D)} = \frac{dC_{N\alpha}}{d(X/D)} * \alpha$$

$$\frac{dC_M}{d(X/D)} = \frac{dC_{M\alpha}}{d(X/D)} * \alpha$$

and

$$C_N = \int_{X_{Start}}^{X_{End}} \frac{dC_N}{d(X/D)} d\frac{X}{D}$$

$$C_N = \int_{X_{Start}}^{X_{End}} \frac{dC_M}{d(X/D)} d\frac{X}{D}$$

Component normal force = $C_N * Q * A_{ref}$

Component pitching moment = $C_M * Q * A_{ref} * D_{ref}$.

These distributed loads do not include the engine shroud loads. The engine shroud contributions are represented by incremental point loads placed at station 4360 or at an X/D of 9.254 (fig. 18). The base of the vehicle is station 4385.5.

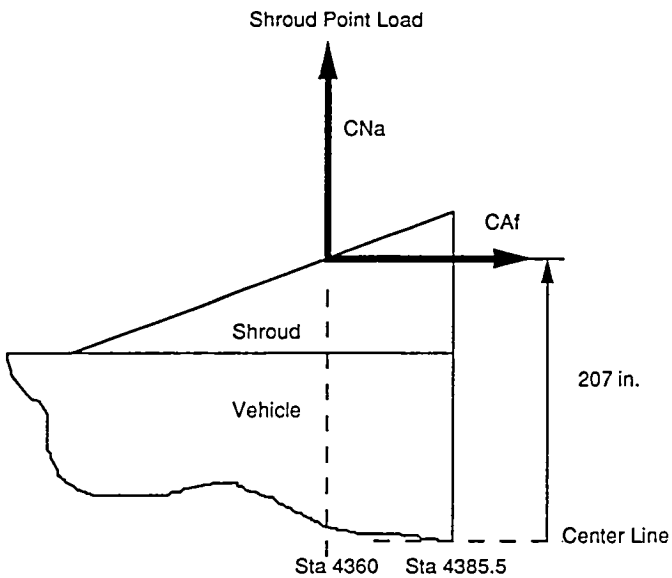

Figure 18. Engine shroud incremental point load placement.

The total normal force and pitching moment are determined using the above formulas and integrating over the whole vehicle, not just a single component, and then adding in the engine shroud increments. For the axial force coefficient, the following formula is used:

$$C_A = \int_{X_{Start}}^{X_{End}} \frac{dC_A}{d(X/D)} d\frac{X}{D} + \Delta C_{A_{Shroud}}$$

To convert to station location multiply the X/D location by D, reference diameter, resulting in length from the nose. It should be noted that integration using the X/D location is required to obtain the correct

total normal force coefficient or axial force coefficient. This is a result of the data being $\frac{dC_{N\alpha}}{d(X/D)}$ and $\frac{dC_A}{d(X/D)}$. Changing dimension formats will result in incorrect integration when using the $C_{N\alpha}$ and C_A values, and new coefficients must be determined to match the new dimensions.

Normal force coefficient slope distribution data, $\frac{dC_{N\alpha}}{d(X/D)}$, pitching moment coefficient slope distribution data, $\frac{dC_{M\alpha}}{d(X/D)}$, and axial force coefficient distribution data, $\frac{dC_A}{d(X/D)}$, for the 1½ stage configuration are given in graphical and tabular formats for the transonic Mach range. Distributed loads for Mach number of 0.6, 0.8, 0.9, 0.95, 1.05, 1.1, 1.25, and 1.46 were determined. This Mach range encompasses the typical maximum dynamic pressure ascent loading conditions. References (5) and (6) also contain data for Mach numbers of 1.96, 2.74, and 3.48. During the NLS program there was no requirement for distributions at these Mach numbers.[8]

Figures 19 through 26 present the normal force coefficient slope distribution data, figures 27 through 34 present the pitching moment coefficient slope distribution data, and figures 35 through 42 present the axial force coefficient distribution data graphically. The distributions are plotted against vehicle caliber's, vehicle station number divided by the reference diameter of the vehicle (*X/D*). These graphic representations were done using a spline function connecting the data points, which resulted in some small localized, undesirable trends between data points. These trends are obvious and should be disregarded. The actual integration and balancing analysis was done using a linear interpolation between the data points. The tabular data corresponding to these distributed loads are presented in appendix B.

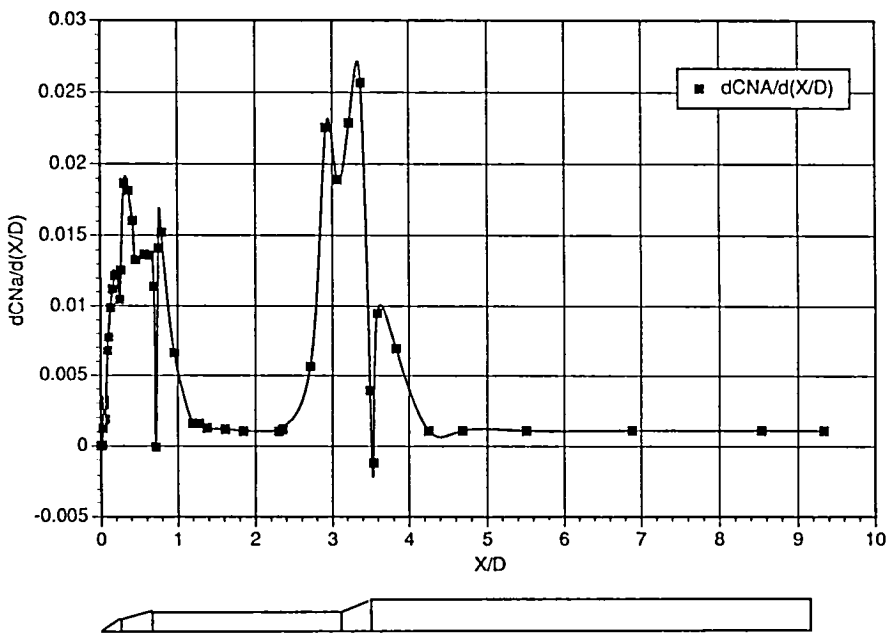

Figure 19. Mach 0.60, $dC_{N\alpha}/d(X/D)$ versus *X/D*.

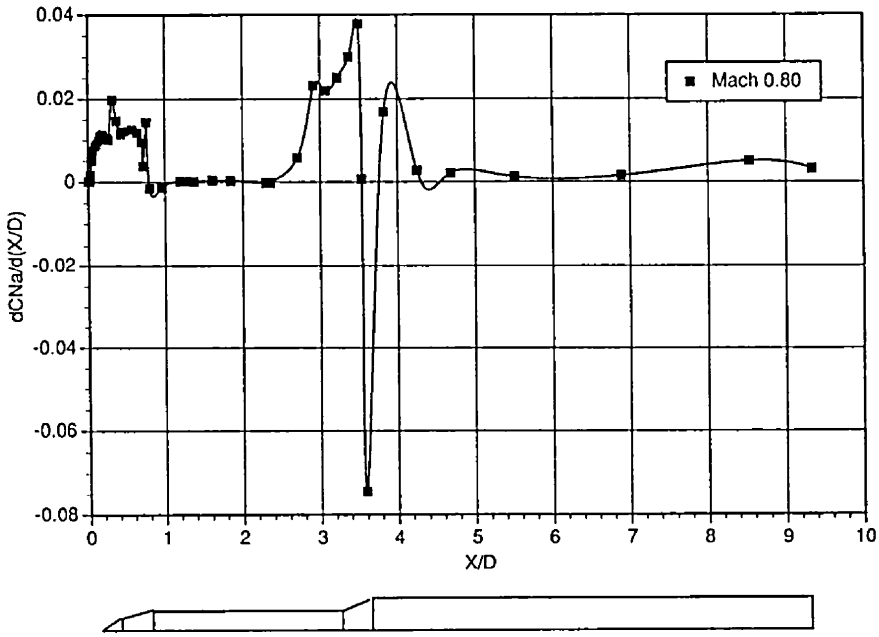

Figure 20. Mach 0.80, $dC_{N\alpha}/d(X/D)$ versus X/D.

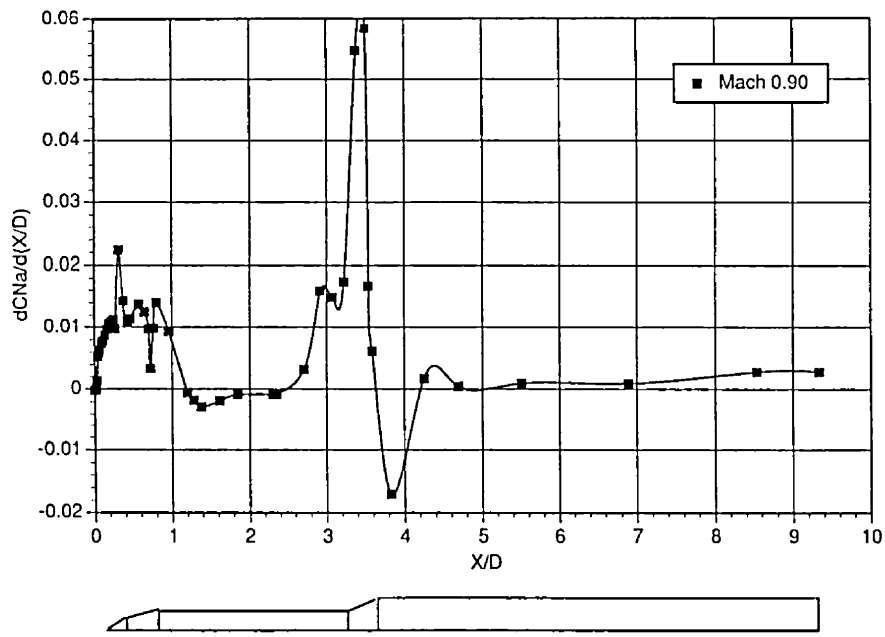

Figure 21. Mach 0.90, $dC_{N\alpha}/d(X/D)$ versus X/D.

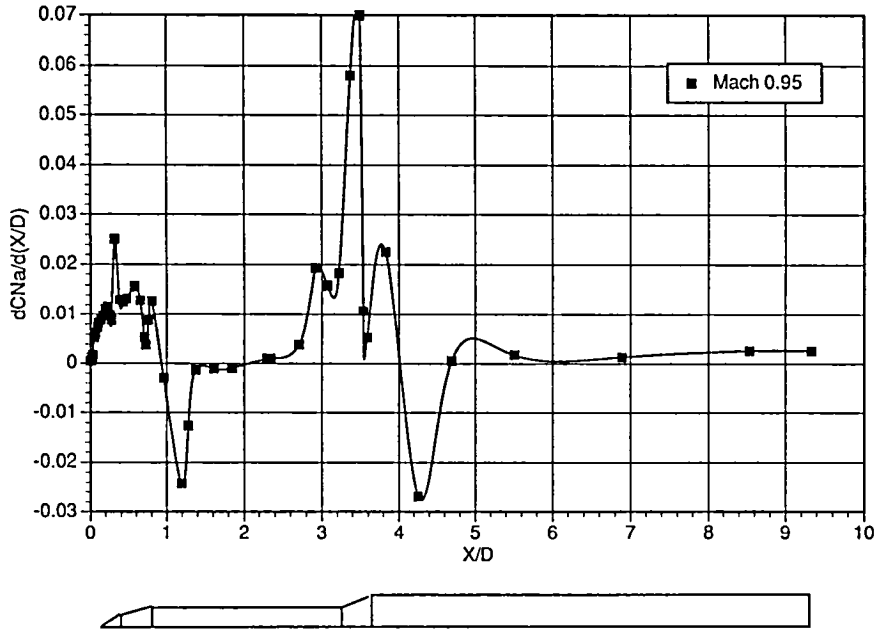

Figure 22. Mach 0.95, $dC_{N\alpha}/d(X/D)$ versus X/D.

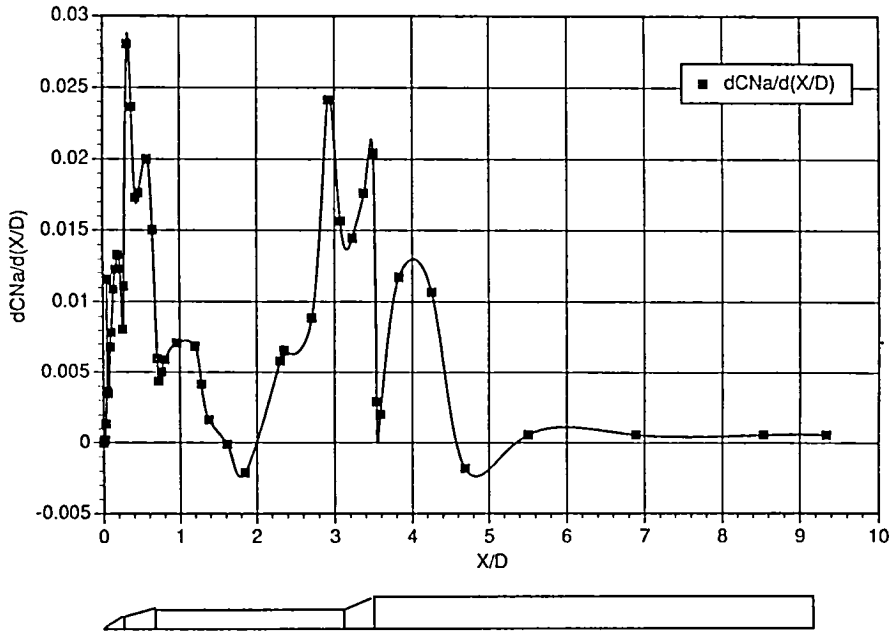

Figure 23. Mach 1.05, $dC_{N\alpha}/d(X/D)$ versus X/D.

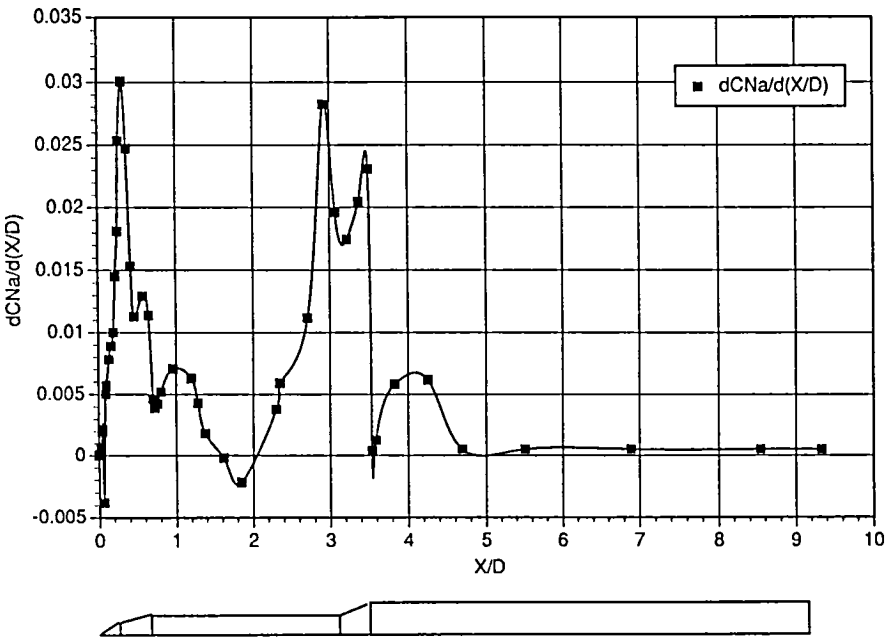

Figure 24. Mach 1.10, $dC_{N\alpha}/d(X/D)$ versus X/D.

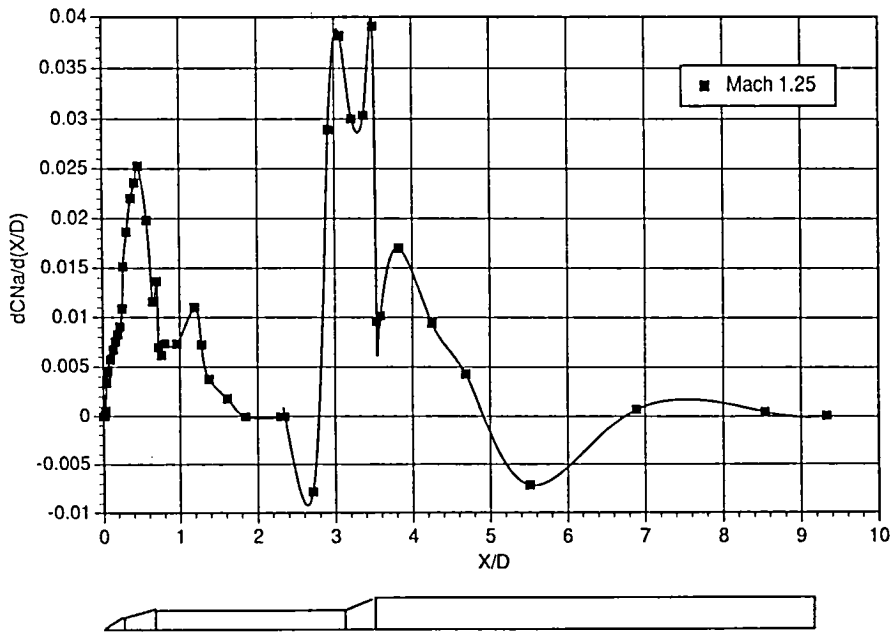

Figure 25. Mach 1.25, $dC_{N\alpha}/d(X/D)$ versus X/D.

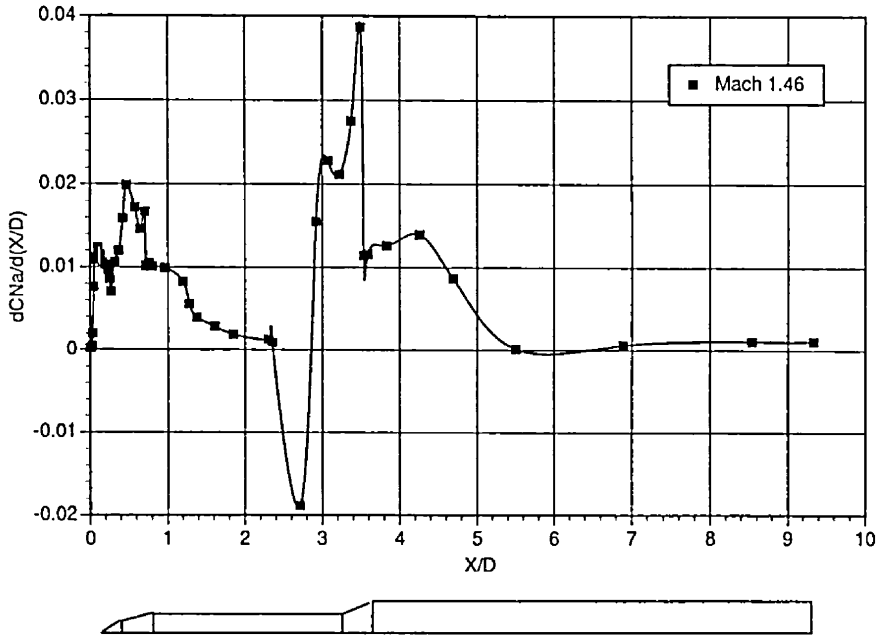

Figure 26. Mach 1.46, $dC_{N\alpha}/d(X/D)$ versus X/D.

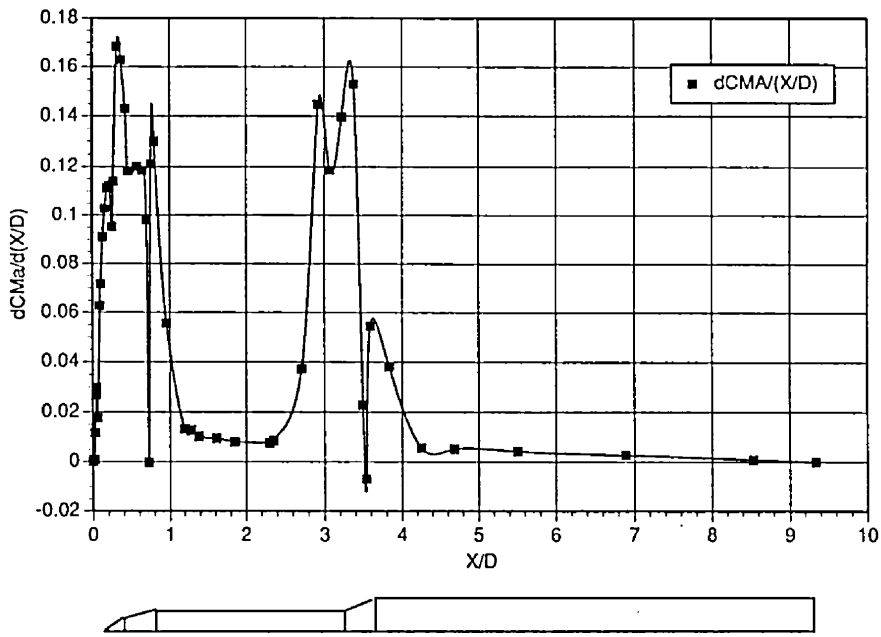

Figure 27. Mach 0.60, $dC_{M\alpha}/d(X/D)$ versus X/D.

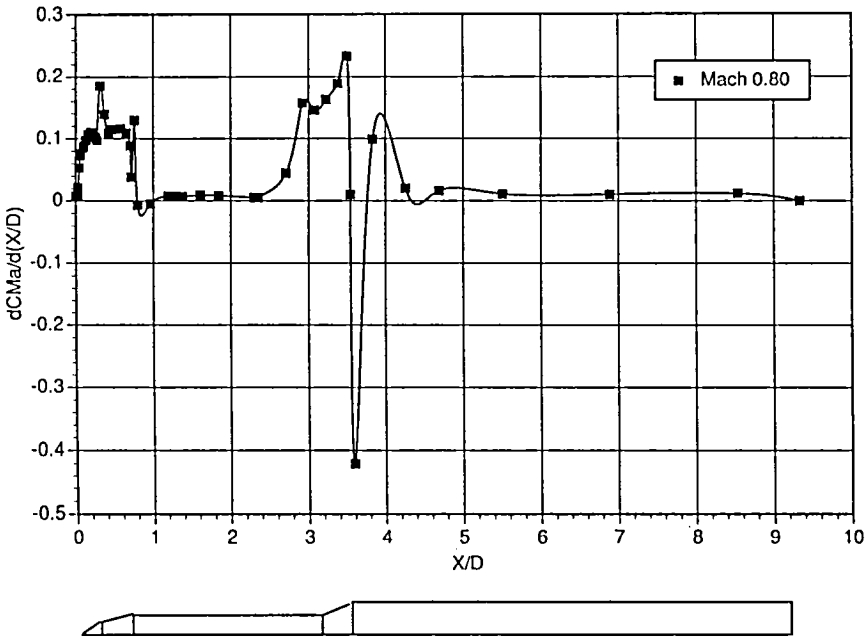

Figure 28. Mach 0.80, $dC_{M\alpha}/d(X/D)$ versus X/D.

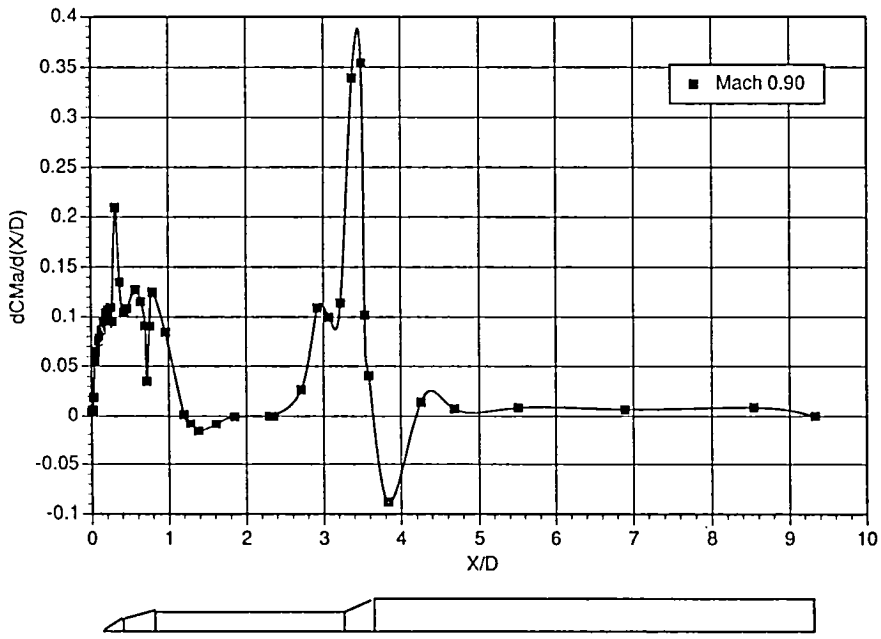

Figure 29. Mach 0.90, $dC_{M\alpha}/d(X/D)$ versus X/D.

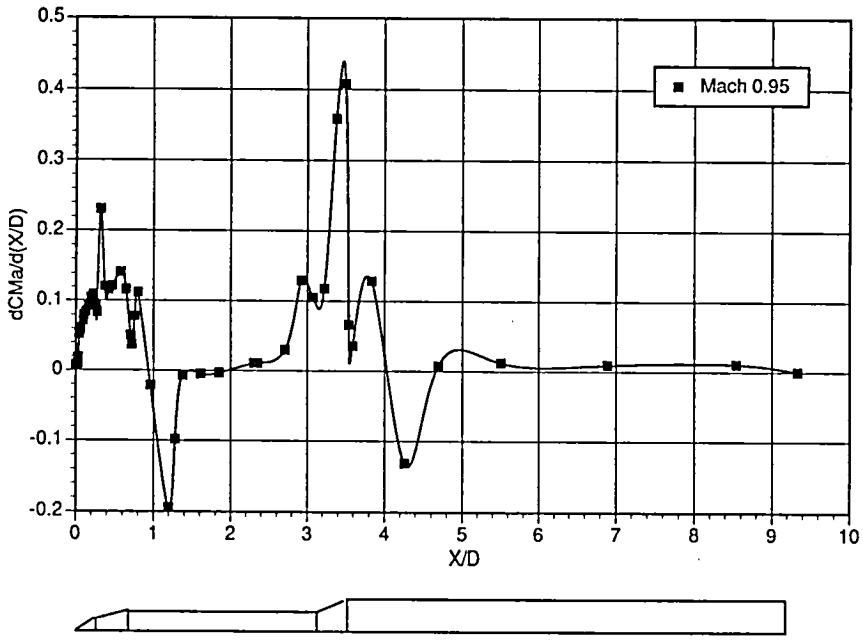

Figure 30. Mach 0.95, $dC_{M\alpha}/d(X/D)$ versus X/D.

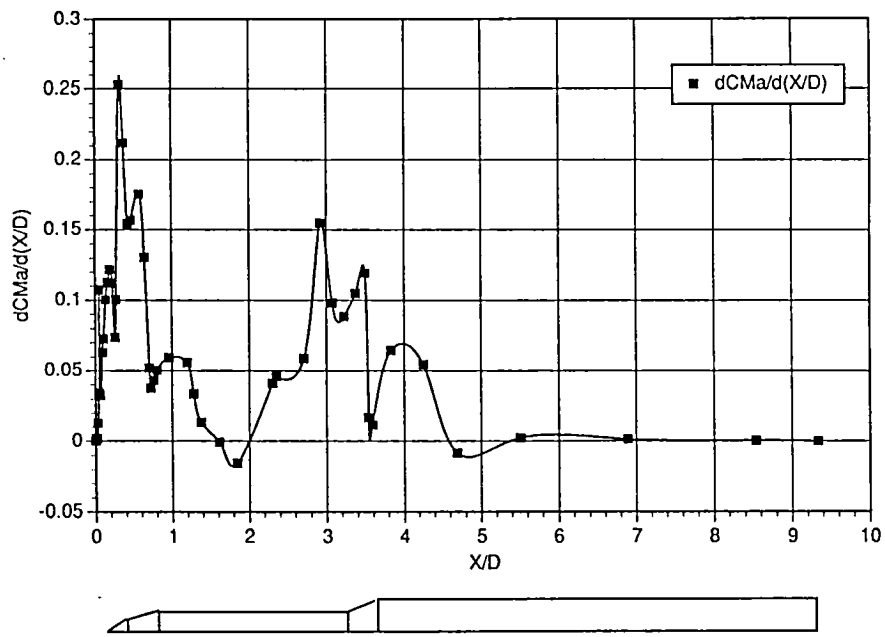

Figure 31. Mach 1.05, $dC_{M\alpha}/d(X/D)$ versus X/D.

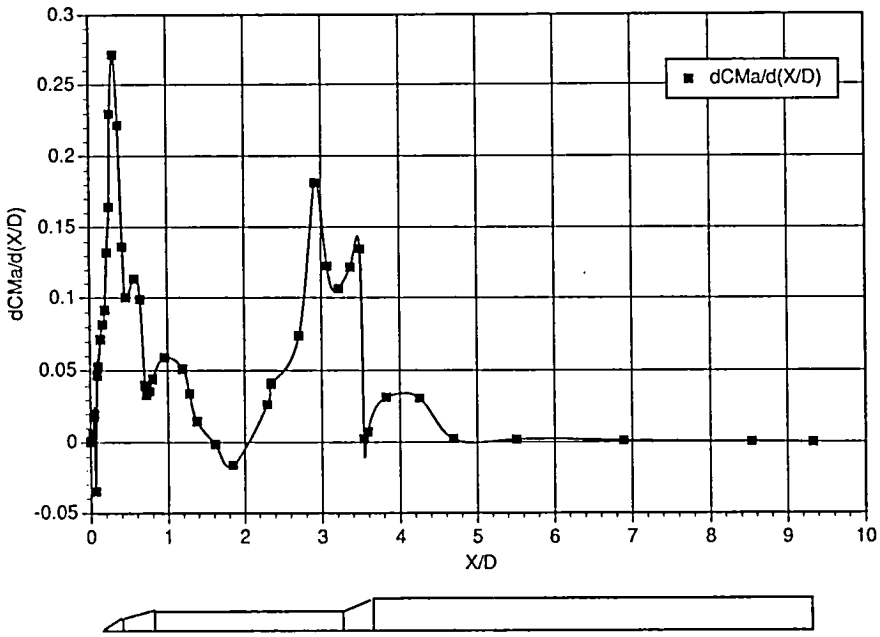

Figure 32. Mach 1.10, $dC_{M\alpha}/d(X/D)$ versus X/D.

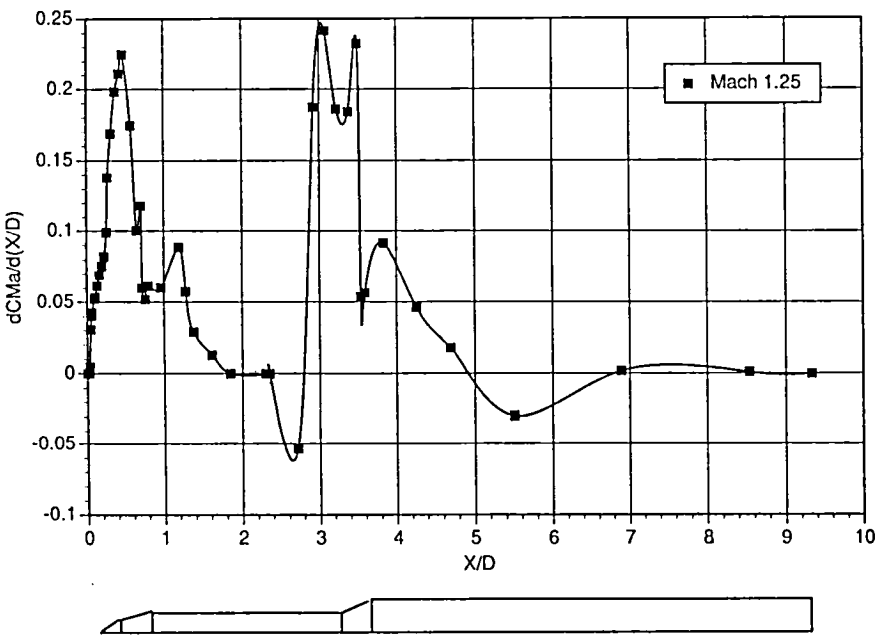

Figure 33. Mach 1.25, $dC_{M\alpha}/d(X/D)$ versus X/D.

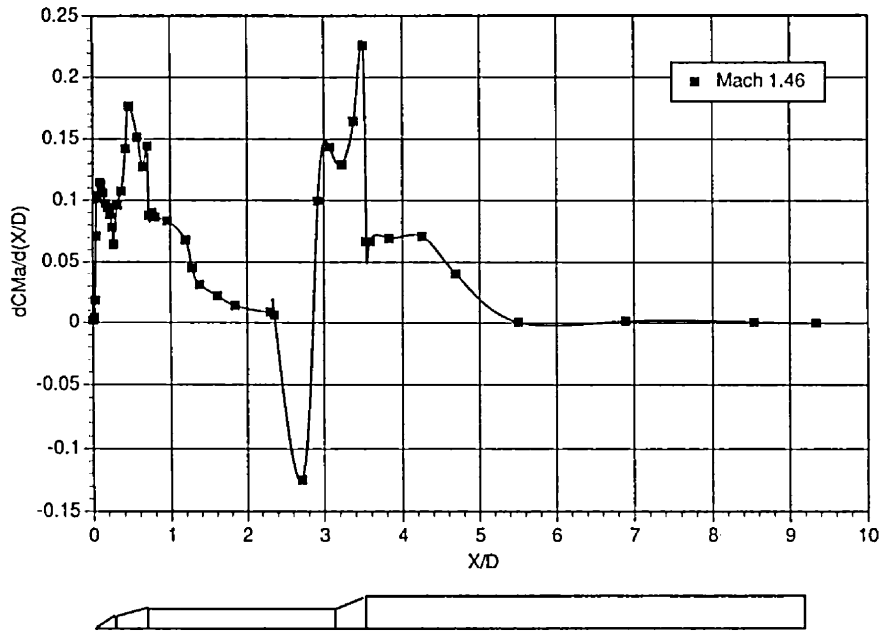

Figure 34. Mach 1.46, $dC_{M\alpha}/d(X/D)$ versus X/D.

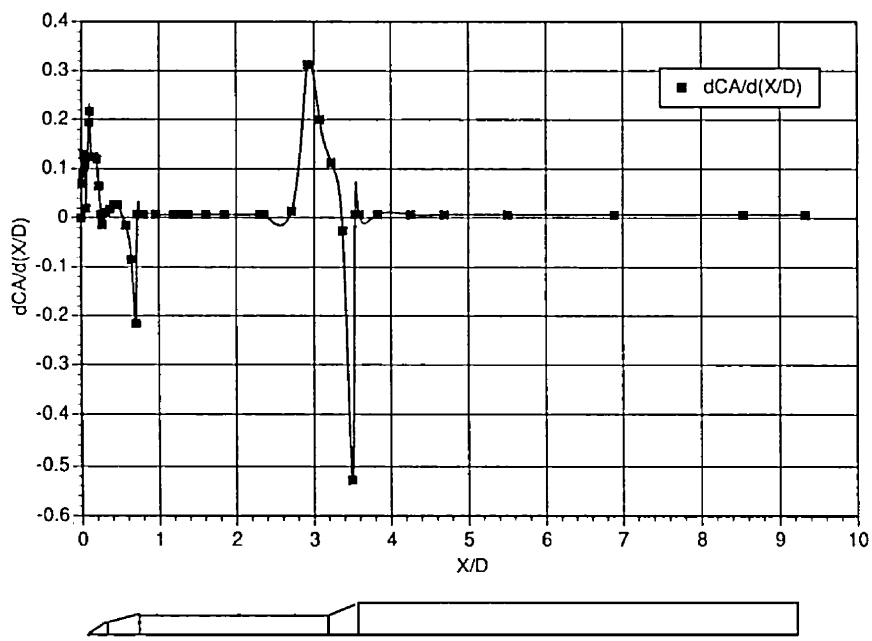

Figure 35. Mach 0.60, $dC_A/d(X/D)$ versus X/D.

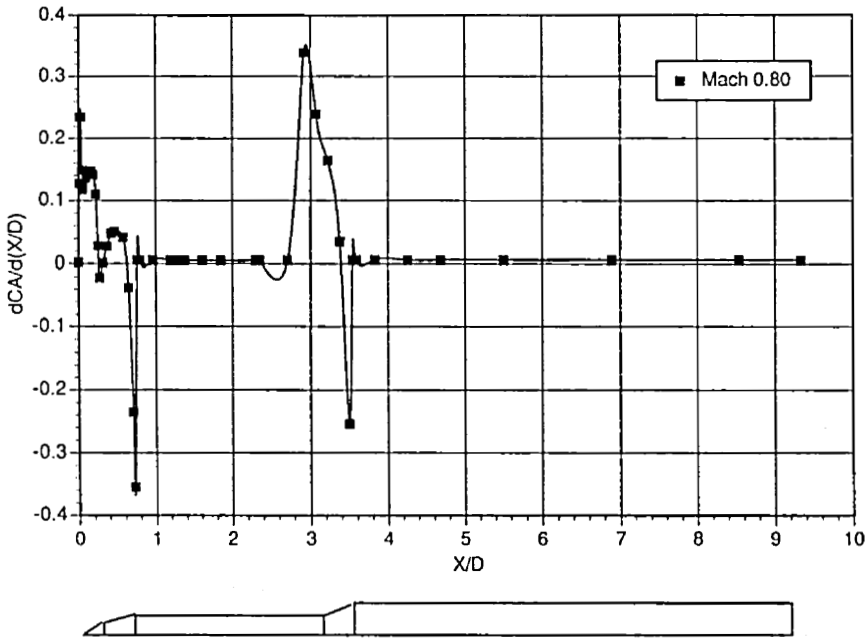

Figure 36. Mach 0.80, $dC_A/d(X/D)$ versus X/D.

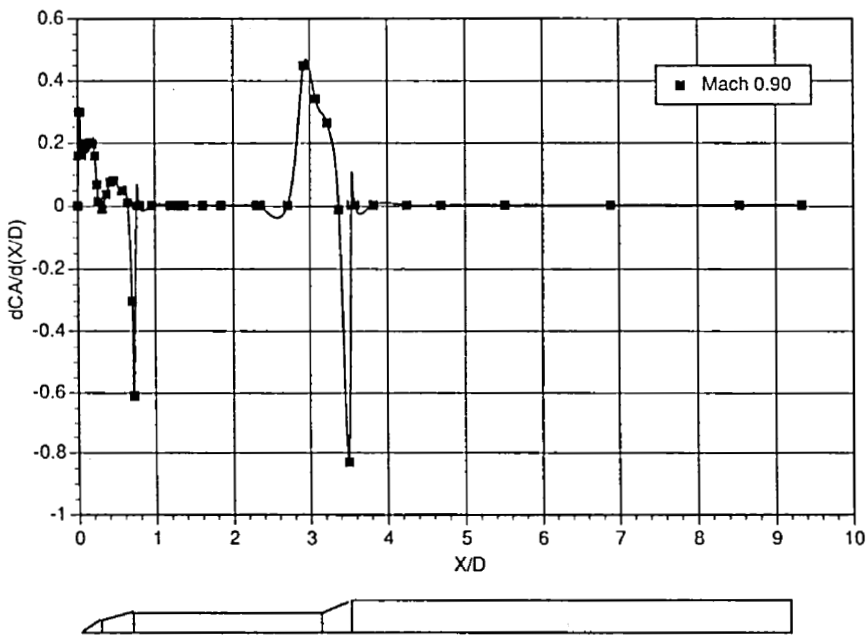

Figure 37. Mach 0.90, $dC_A/d(X/D)$ versus X/D.

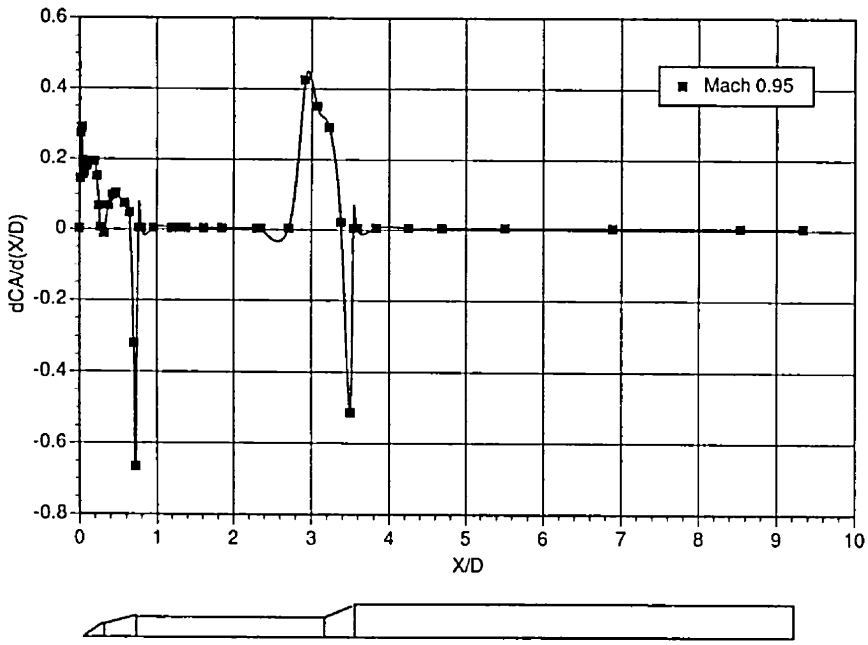

Figure 38. Mach 0.95, $dC_A/d(X/D)$ versus X/D.

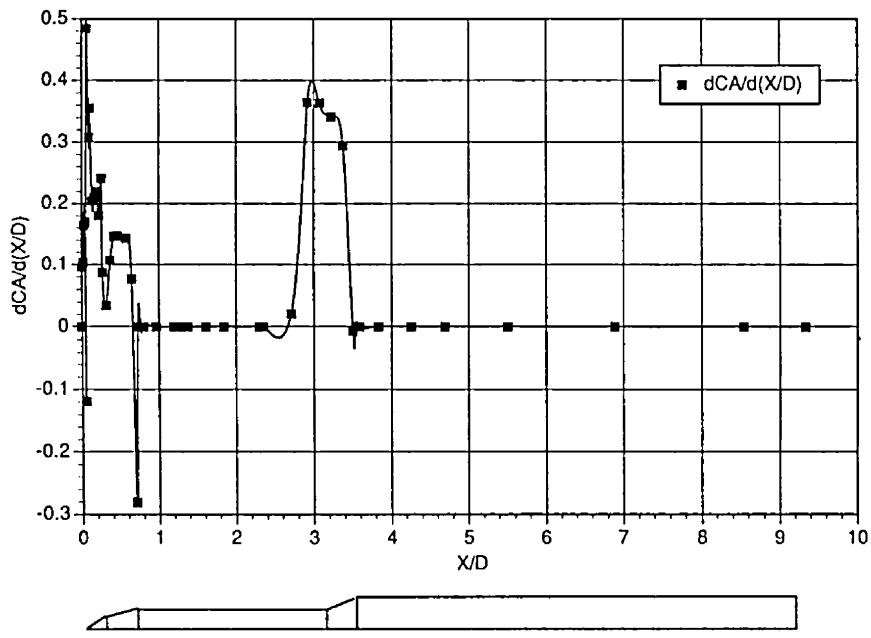

Figure 39. Mach 1.05, $dC_A/d(X/D)$ versus X/D.

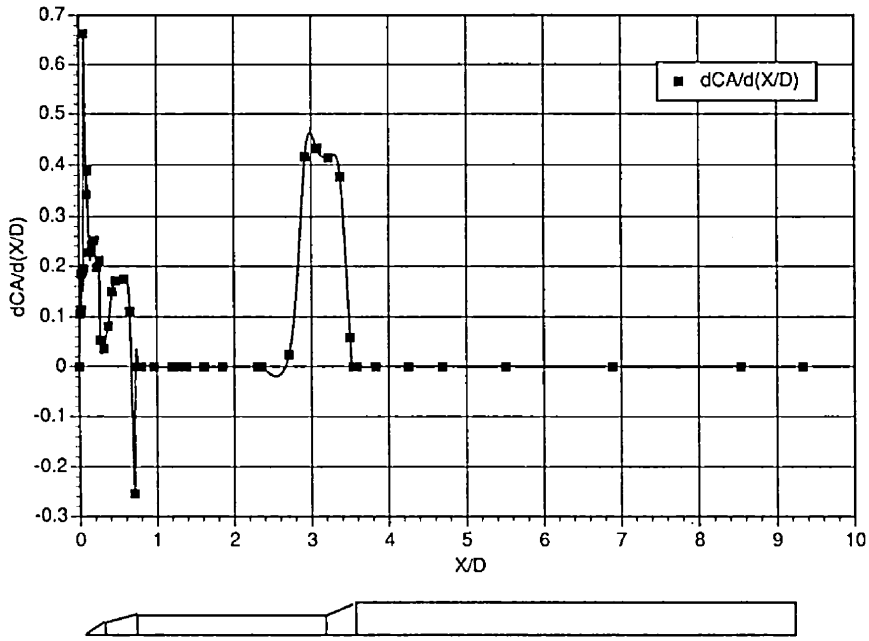

Figure 40. Mach 1.10, $dC_A/d(X/D)$ versus X/D.

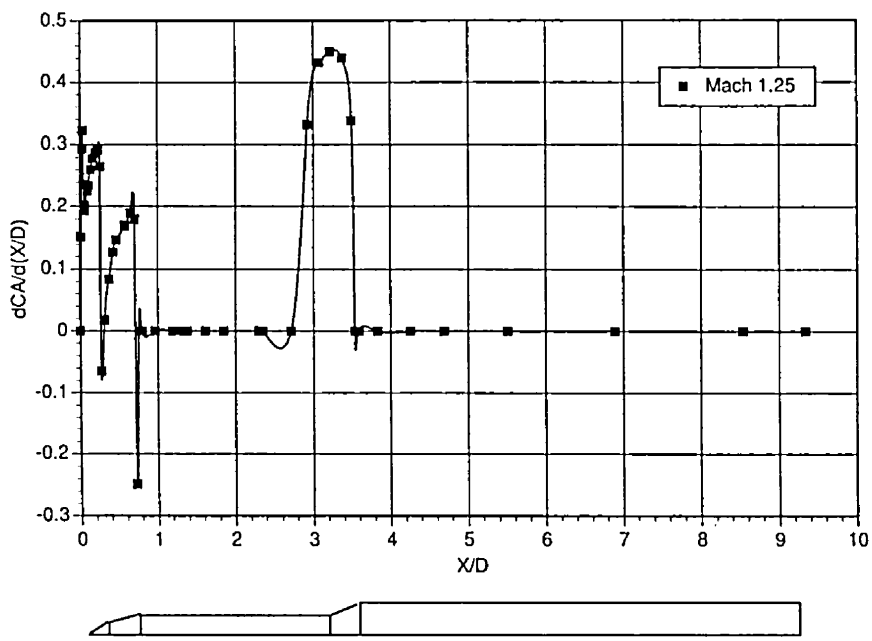

Figure 41. Mach 1.25, $dC_A/d(X/D)$ versus X/D.

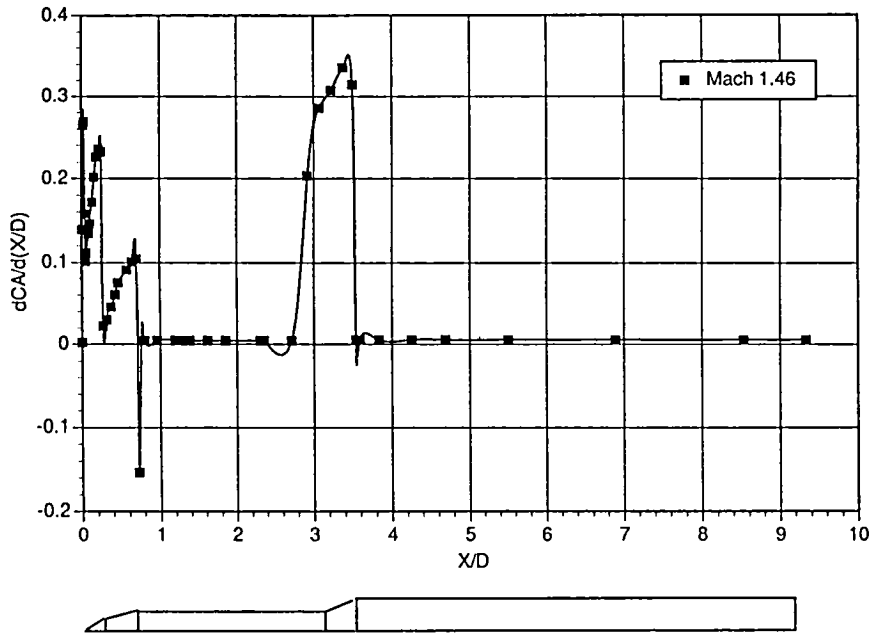

Figure 42. Mach 1.46, $dC_A/d(X/D)$ versus X/D.

The shroud increments given at the bottom of the distribution tables were determined from reference (8) and are added to the distribution totals to obtain the total coefficient loads for the vehicle including shrouds. The shroud increments are for four shrouds. These increments are applied at station 4360 or at an X/D of 9.254 (fig. 18).

VII. CONCLUSIONS

These two wind tunnel tests, in support of the detailed configuration definition, were conducted in the NASA MSFC's 14×14-Inch TWT during 1992. The static stability and a pressure test each utilized 0.004-scale models. The static stability test resulted in the forces and moments acting on the vehicle. The aerodynamics for the reference configuration with and without feedlines and an evaluation of three proposed engine shroud configurations were also determined. The pressure test resulted in pressure distributions over the reference vehicle with and without feedlines, including the reference engine shrouds. These pressure distributions were integrated and balanced to the static stability coefficients, resulting in distributed aerodynamic loads on the vehicle. The wind tunnel tests covered a Mach range of 0.60 to 4.96.

The location and geometry of the engine shrouds tested is shown in figure 43. A set of four shrouds at 45° spacing were mounted to the vehicle for each configuration. The effects of the three engine shrouds on the longitudinal aerodynamic characteristics of the 1½ stage configuration are shown in figures 44 through 46. From these figures it is seen that the larger the shroud angle, the greater increase in drag. A 15-percent decrease in total vehicle drag can be seen by using an optimum aerodynamic engine shroud design. This optimum design is based on vehicle aerodynamics, engine hinge moment requirements, and vehicle geometry constraints.

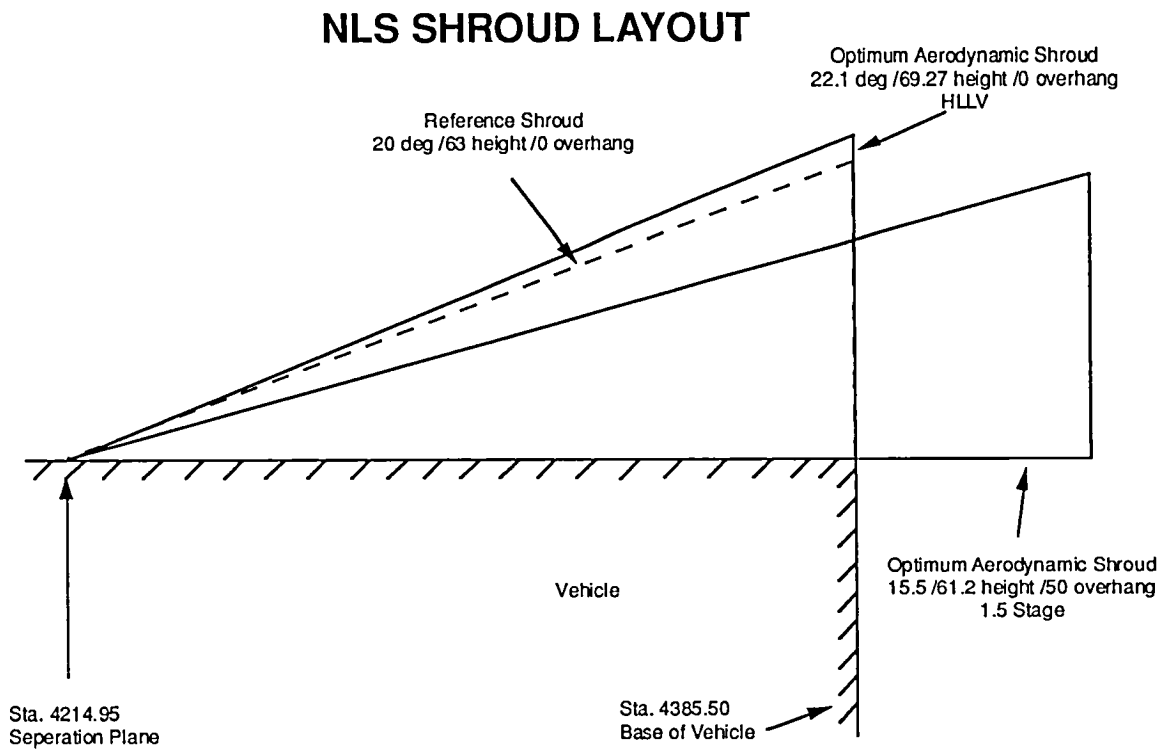

Figure 43. Engine shroud location and geometry.

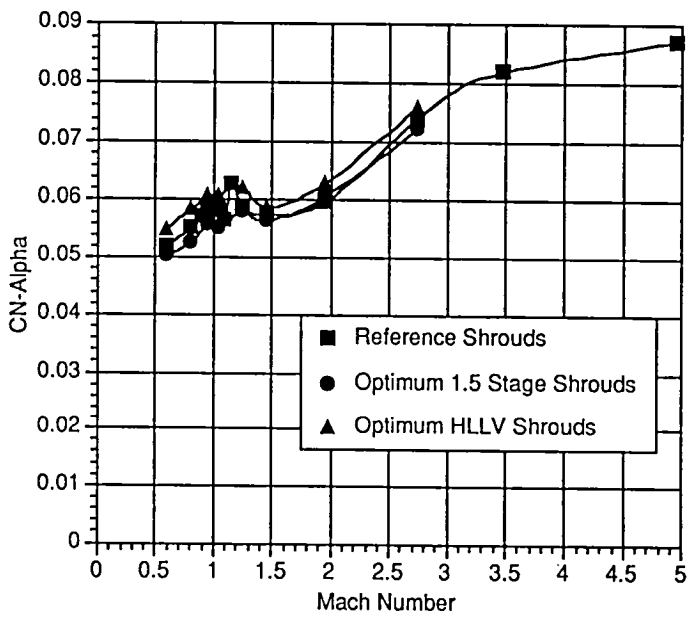

Figure 44. Engine shroud comparison $C_{N\alpha}$ versus Mach.

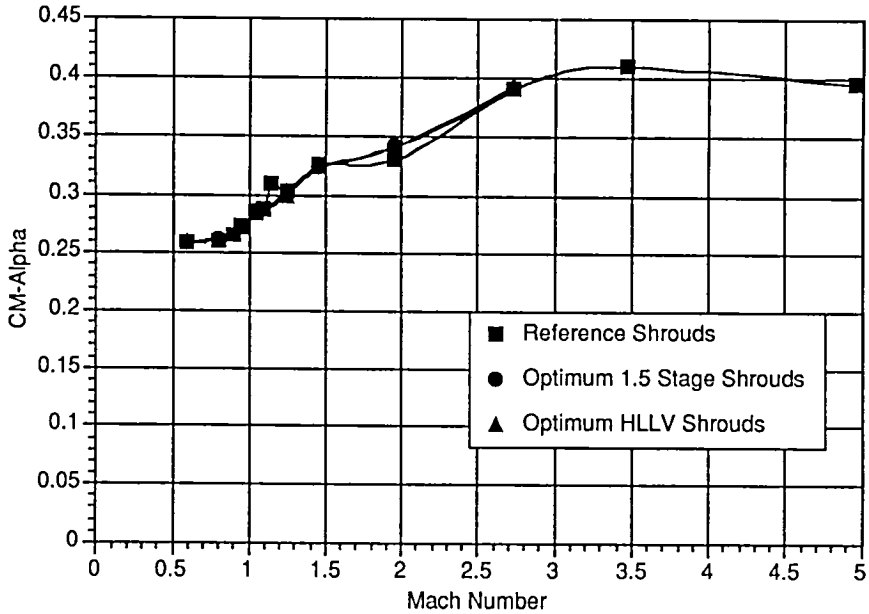

Figure 45. Engine shroud comparison $C_{M\alpha}$ versus Mach.

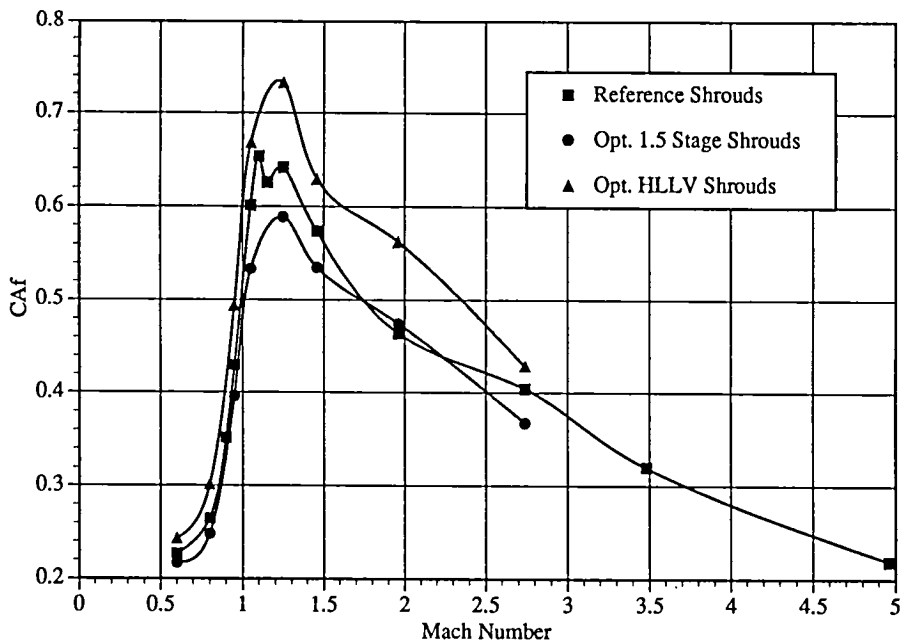

Figure 46. Engine shroud comparison C_{Af} versus Mach.

The effects of feedlines, reference engine shrouds, and their component increments on the aerodynamic characteristics are shown in figure 47 through 52. Feedlines have little effect on vehicle drag when compared to the effect of engine shrouds, which is approximately 25 percent of the total vehicle drag. Feedlines, on the other hand, have a relatively large effect on the lateral characteristics of the vehicle. The effect of feedlines and shrouds on the center of pressure on the vehicle is shown in figure 52. The clean vehicles' center of pressure is moved aft with addition of feedlines and engine shrouds. The engine shrouds account for most of this movement aft.

The NLS aerodynamic data was used by the Trajectory and Performance Group, the Loads Analysis Group, and the Guidance and Control Group at MSFC in the design study of the 1½ stage vehicle. This data is applicable for use to other similar configuration that may be developed.

The data bases resulting from the wind tunnel tests performed at the MSFC's 14×14-Inch TWT provide the basis for detailed vehicle analysis. They also provide a generic matrix of data on a symmetric inline launch vehicle. The full data base also provides increments for engine shroud and feedline effects. These data, the data base and incremental data, when combined with the distributed loads provide a firm basis for analytical programs or computational fluid dynamic benchmark studies over the full range of subsonic, transonic, and supersonic Mach numbers. Future tests and studies can benefit from the data generated from these tests.

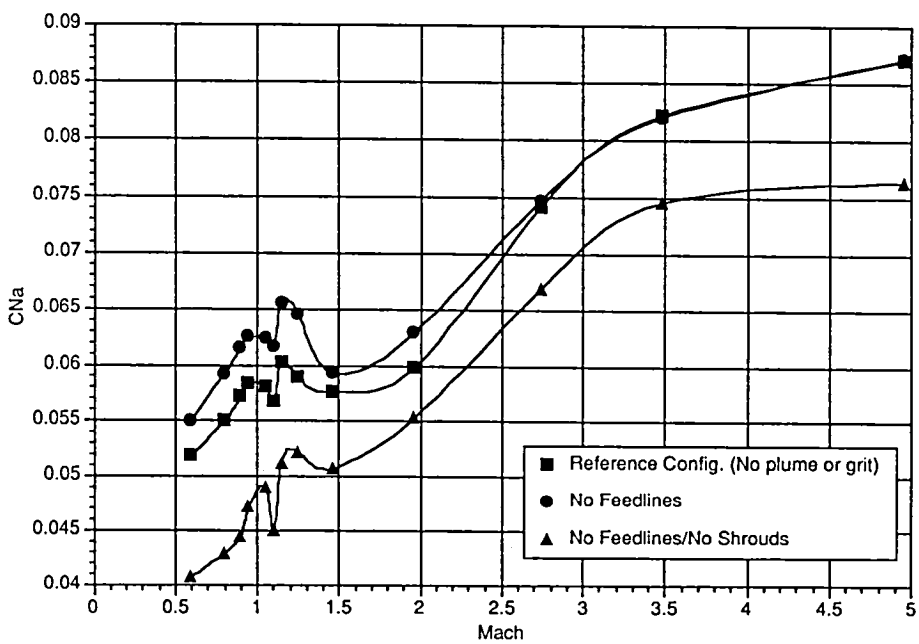

Figure 47. Comparison plot of $C_{N\alpha}$ versus Mach.

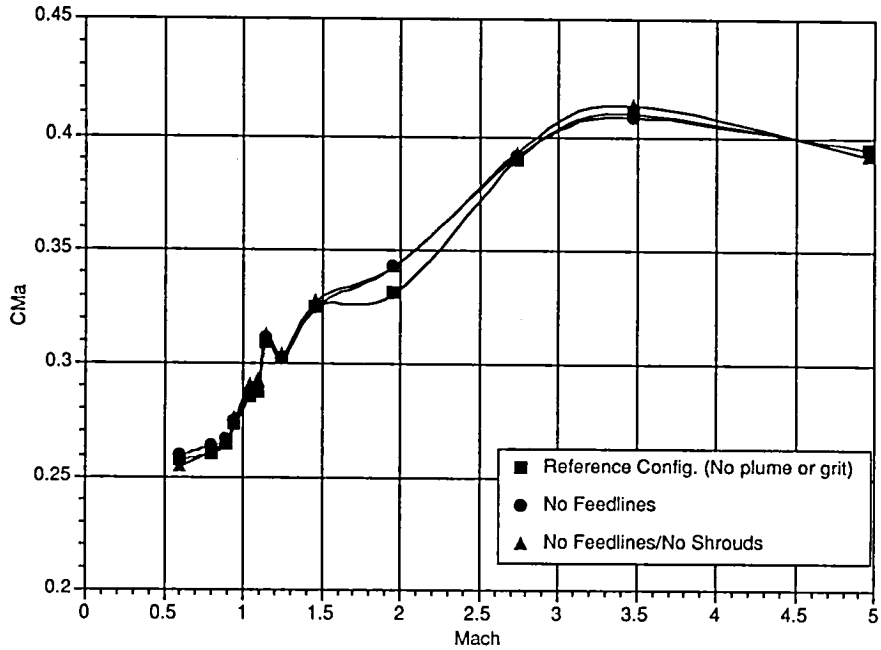

Figure 48. Comparison plot of $C_{M\alpha}$ versus Mach.

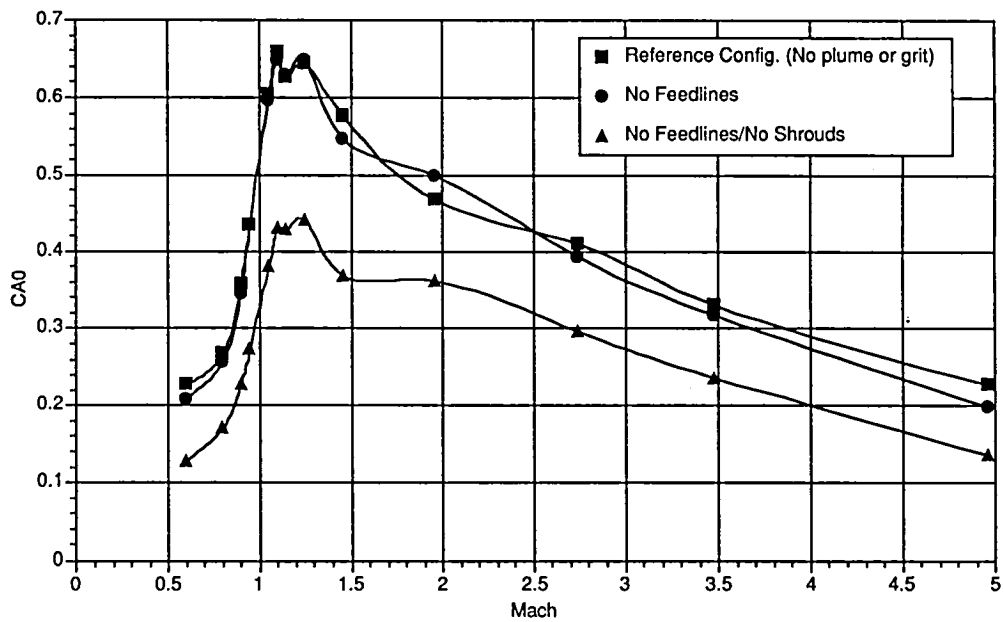

Figure 49. Comparison plot of C_{Ao} versus Mach.

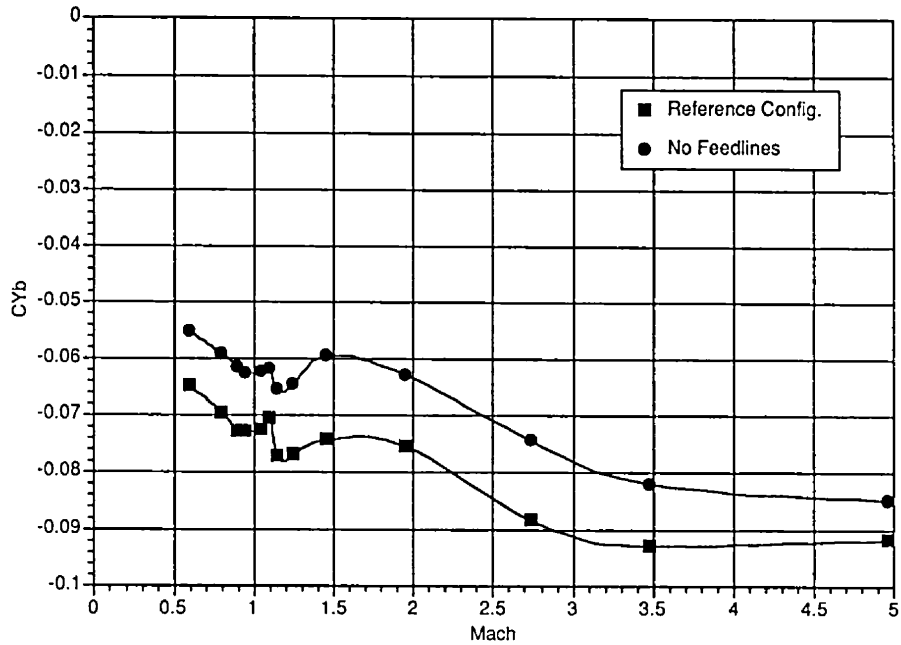

Figure 50. Vehicle with/without feedlines comparison $C_{Y\beta}$ versus Mach.

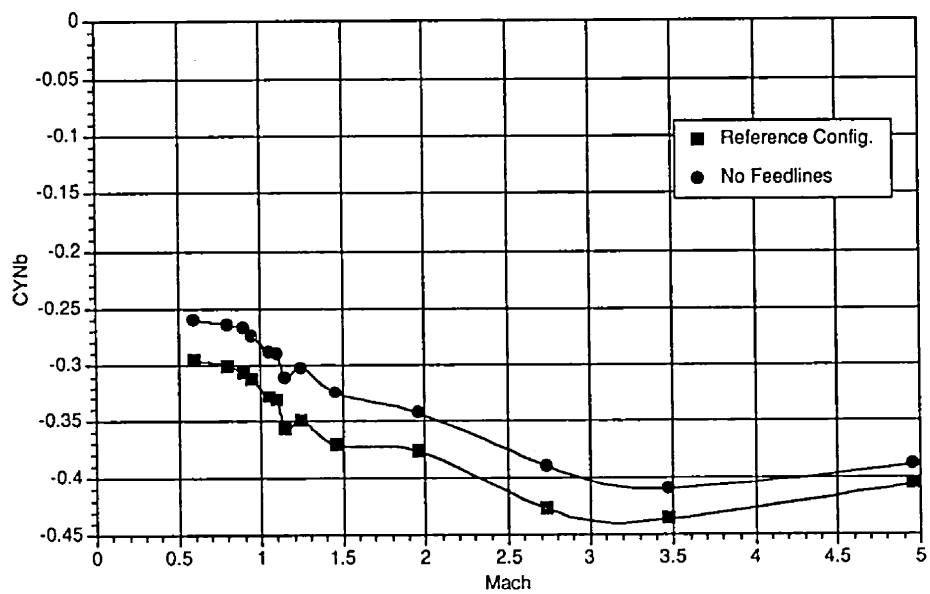

Figure 51. Vehicle with/without feedlines comparison $C_{l\beta}$ versus Mach.

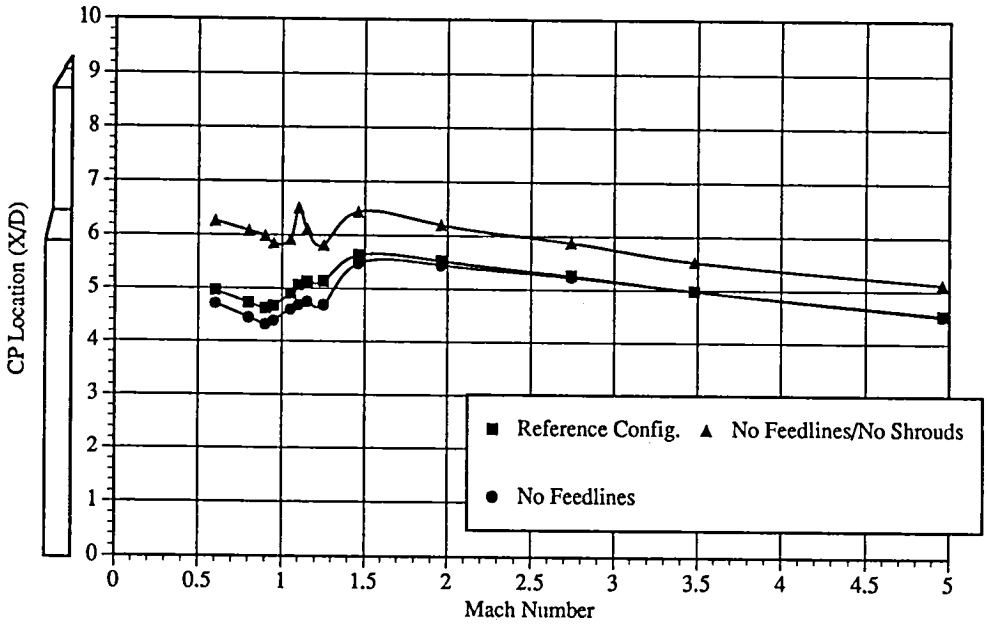

Figure 52. Comparison of variation of center of pressure versus Mach.

REFERENCES

1. National Launch System (NLS) Reference System Definition. EE81(026-91), May 28, 1991.

2. Simon, E.: "The George C. Marshall Space Flight Center's 14×14-Inch Trisonic Wind Tunnel Technical Handbook." NASA TM X-64624, November 5, 1971.

3. Pokora, D.C., and Springer, A.M.: "A Shadowgraph Study of the National Launch System 1½ Stage and Heavy Lift Launch Vehicle Configurations." NASA RP-TBD, 1994.

4. Springer, A.M.: "Experimental Investigation of Plume Induced Flow Separation on the National Launch System (NLS) 1½ Stage Launch Vehicle." AIAA 94-0030, January, 1994.

5. Pokora, D.C.: "Posttest Report for the National Launch System (NLS) in the MSFC 14-Inch Trisonic Wind Tunnel." ED34-04-93, March 12, 1993.

6. Springer, A.M.:."Post-Test Report for TWT 734 The National Launch System (NLS) 1½ Stage Pressure Test in the MSFC 14-Inch Trisonic Wind Tunnel." ED35-127-92, September 3, 1992.

7. Springer, A.M.: "National Launch System (NLS) 1½ Stage Distributed Loads." ED35-152-92, December 8, 1992.

8. Pokora, D.C.: "Update to the Aerodynamic Database for the 1½ Stage Configuration for the National Launch System." ED35-83-92, June 5, 1992.

APPENDIX A

STATIC STABILITY DATA BASE

1.5 STAGE REFERENCE CONFIGURATION w/Plumes

COEFF/MACH	0	0.6	0.8	0.9	0.95	1.05	1.1
CNa	0.05	0.051638	0.052973	0.053234	0.054478	0.056068	0.055539
CMa	0.258425	0.258425	0.259746	0.262482	0.271271	0.286673	0.289559
CYb	–0.0599	–0.064256	–0.067568	–0.068456	–0.069352	–0.070798	–0.069871
CYNb	–0.28	–0.293771	–0.297957	–0.301729	–0.309866	–0.329174	–0.333979
CBLb	0	0	0	0	0	0	0
CA0	0.2	0.221529	0.255329	0.323363	0.380371	0.524	0.575746

1.15	1.25	2.46	1.96	2.74	3.48	4.96
0.058527	0.057911	0.056917	0.061311	0.0717236	0.07439906	0.06947641
0.309339	0.303354	0.326607	0.342068	0.383663	0.3936375	0.3738235
–0.076712	–0.07656	–0.07395	–0.078046	–0.08630272	–0.08885967	–0.06938145
–0.358316	–0.350907	–0.371529	–0.38846	–0.4204563	–0.431989	–0.3812833
0	0	0	0	0	0	0
0.553637	0.578022	0.499793	0.448496	0.3865777	0.3223577	0.1752813

MACH	ALT (ft)	Q (pfs)	THRST (lbs)	FAB (lbs)
0	0	0	0	0
0.61	9,767	384.2	3,491,867	37,977.7
0.8	14,926	547.3	2,913,900.75	41,119.57
0.9	19,231	584.8	2,965,691.25	41,767.07
0.94	21,062	599.1	2,985,669.25	42,414.58
1.07	25,916	625.3	3,033,270.5	43,758.52
1.12	27,967	630.1	3,051,234.25	40,911.27
1.17	30,080	633.9	3,068,509.25	36,687.49
1.26	33,371	638.9	3,093,054	29,509.55
1.41	37,944	639.9	3,123,076.25	15,380.07
1.66	45,454	620.7	3,161,505.75	5,990.87
2.02	56,381	526	3,199,134.25	–5,181.3
2.19	62,254	460.3	3,212,174.25	–10,468.95
2.49	73,142	350.8	3,227,807	–15,889.43
2.71	81,363	281.2	3,234,955.5	–15,447.31
2.99	91,684	213.7	3,240,632.25	–13,295.85
3.43	108,017	136	3,244,574	–9,773.67
3.78	121,351	93.7	3,247,423	–7,554.01
4.16	135,170	65.2	3,248,522.75	–6,186.5
4.52	145,375	51.1	3,899,016.25	–6,176.2
5.01	158,136	38.6	3,899,394	–4,890.88

APPENDIX B

DISTRIBUTED LOADS

NLS 1 1/2 Stage Airloads Distribution Mach 0.6			
Aref=594 ft^2		Dref=330.0 in	
x/d	dCA/d(X/D)	dCNa/d(X/D)	dCMa/d(X/D)
0	0	0	0
0.009	0.07	9.43E-05	0.00087943
0.021	0.091003	9.43E-05	0.0008783
0.03	0.12962	0.0012575	0.011697
0.045	0.10962	0.0029045	0.026973
0.051	0.115	0.0032	0.029698
0.06	0.019547	0.001898	0.017597
0.091	0.19435	0.0067963	0.062802
0.103	0.21606	0.0077525	0.071544
0.133	0.1234	0.0099133	0.091188
0.163	0.12412	0.011215	0.10283
0.194	0.11877	0.012164	0.11115
0.224	0.064693	0.012305	0.11207
0.254	0.006953	0.010503	0.095342
0.27	-0.013996	0.01257	0.1139
0.315	0.010828	0.018673	0.16837
0.37	0.017893	0.018166	0.1628
0.424	0.027142	0.016056	0.14302
0.466	0.025965	0.013333	0.11821
0.576	-0.015557	0.013713	0.12006
0.648	-0.084254	0.013652	0.11855
0.703	-0.21509	0.011389	0.098271
0.722	0.007	-3.87E-05	-0.0003329
0.76	0.007	0.014136	0.12117
0.8	0.007	0.015239	0.13002
0.96	0.007	0.0066525	0.055692
1.194	0.007	0.0016295	0.01326
1.28	0.007	0.0015858	0.012768
1.376	0.007	0.0012948	0.010301
1.61	0.007	0.0012198	0.009419
1.845	0.007	0.0010827	0.0081055
2.3	0.007	0.0010845	0.0076257
2.35	0.007	0.0012202	0.0085187
2.709	0.013927	0.0056503	0.03742
2.921	0.31279	0.022559	0.14462
3.073	0.20027	0.01895	0.1186
3.224	0.11296	0.0229	0.13986
3.376	-0.025481	0.0257	0.15306
3.497	-0.52777	0.0039365	0.022968
3.539	0.007	-0.0011808	-0.0068401
3.588	0.007	0.009492	0.054518
3.83	0.007	0.0069542	0.038259
4.254	0.007	0.0011073	0.0056226
4.688	0.007	0.0011073	0.005142
5.506	0.007	0.0011073	0.0042362
6.891	0.007	0.0011168	0.0027257
8.536	0.007	0.0011168	0.00088852
9.332	0.007	0.0011168	0
total	0.132499	0.039271	0.254319
shrouds	0.079978	0.014386	0.004861
total w/ shrds	0.212477	0.053657	0.25918

NLS 1 1/2 Stage Airloads Distribution Mach 0.8			
Aref=594. ft**2		Dref=330.0 in	
X/D	dCA/d(X/D)	dCNa/d(X/D)	dCMa/d(X/D)
0	0.00244	0.00014	0.00665
0.009	0.12727	0.00014	0.00665
0.021	0.2352	0.00042	0.00924
0.03	0.23464	0.00168	0.02104
0.045	0.14853	0.00514	0.05323
0.051	0.11688	0.00727	0.07301
0.06	0.12096	0.00762	0.07625
0.091	0.13507	0.00864	0.08559
0.103	0.13969	0.009	0.08877
0.133	0.14545	0.00995	0.09738
0.163	0.14689	0.01097	0.1066
0.194	0.14094	0.01144	0.11063
0.224	0.1099	0.01052	0.10189
0.254	0.02826	0.0106	0.10238
0.27	-0.02186	0.01015	0.09811
0.315	0.00173	0.0198	0.18491
0.37	0.02811	0.01477	0.13857
0.424	0.048	0.01156	0.10904
0.466	0.05067	0.01222	0.1145
0.576	0.04181	0.01257	0.11629
0.648	-0.03823	0.01195	0.11004
0.703	-0.23487	0.00959	0.08886
0.722	-0.35494	0.00378	0.03822
0.76	0.00499	0.01441	0.12892
0.8	0.00499	-0.00143	-0.00682
0.96	0.00499	-0.00127	-0.00522
1.194	0.00499	0.00022	0.00727
1.28	0.00499	0.00021	0.00718
1.376	0.00499	0.00019	0.00698
1.61	0.00499	0.00039	0.00856
1.845	0.00499	0.00038	0.00839
2.3	0.00499	0.00066	0.00466
2.35	0.00499	0.00067	0.00468
2.709	0.00499	0.00582	0.04422
2.921	0.33824	0.0232	0.15666
3.073	0.23904	0.02197	0.14563
3.224	0.16399	0.02514	0.16242
3.376	0.03548	0.03007	0.189
3.497	-0.25354	0.03791	0.23266
3.539	0.00619	0.00069	0.00983
3.588	0.00619	-0.07426	-0.42072
3.83	0.00619	0.01691	0.09889
4.254	0.00619	0.00276	0.01993
4.688	0.00619	0.00217	0.01607
5.506	0.00619	0.00125	0.01086
6.891	0.00619	0.00155	0.01008
8.536	0.00619	0.005	0.01171
9.332	0.00619	0.00319	0.01171
Total	0.17723	0.03765	0.26026
Shrouds	0.08706	0.01629	0.00269
Total	0.26429	0.05394	0.26295

NLS 1 1/2 Stage Airloads Distribution Mach 0.9			
Aref=594. ft**2		Dref=330.0 in	
X/D	dCA/d(X/D)	dCNa/d(X/D)	dCMa/d(X/D)
0	0.00071	0.00042	0.00389
0.009	0.16041	0.00042	0.00389
0.021	0.29849	0.00071	0.00658
0.03	0.29757	0.00134	0.01886
0.045	0.20043	0.00529	0.05569
0.051	0.16205	0.00598	0.06209
0.06	0.16719	0.0063	0.06504
0.091	0.18367	0.0074	0.0751
0.103	0.18918	0.00779	0.0786
0.133	0.1963	0.00866	0.08648
0.163	0.20304	0.00967	0.09556
0.194	0.1968	0.0106	0.10395
0.224	0.16039	0.01098	0.10719
0.254	0.06902	0.01124	0.10929
0.27	0.01459	0.00973	0.0953
0.315	-0.00951	0.02233	0.20882
0.37	0.03881	0.01428	0.13505
0.424	0.07684	0.01096	0.10454
0.466	0.081	0.01146	0.10856
0.576	0.04984	0.01371	0.1272
0.648	0.01164	0.0125	0.11569
0.703	-0.30121	0.00972	0.09086
0.722	-0.60863	0.00335	0.03535
0.76	0.00277	0.00985	0.09062
0.8	0.00277	0.01391	0.1248
0.96	0.00277	0.00936	0.08445
1.194	0.00277	-0.00053	-0.00431
1.28	0.00277	-0.00176	-0.00817
1.376	0.00277	-0.00279	-0.01621
1.61	0.00277	-0.00189	-0.00866
1.845	0.00277	-0.00089	-0.00081
2.3	0.00277	-0.00087	-0.00035
2.35	0.00277	-0.00087	-0.00032
2.709	0.00277	0.00319	0.02675
2.921	0.44857	0.01587	0.10884
3.073	0.34154	0.01479	0.09978
3.224	0.26334	0.01742	0.11411
3.376	-0.01074	0.05473	0.33907
3.497	-0.82844	0.05838	0.3549
3.539	0.00397	0.01667	0.10198
3.588	0.00397	0.00617	0.04083
3.83	0.00397	-0.01698	-0.08804
4.254	0.00397	0.00173	0.01404
4.688	0.00397	0.00047	0.00728
5.506	0.00397	0.00095	0.00853
6.891	0.00397	0.00091	0.00677
8.536	0.00397	0.00279	0.00883
9.332	0.00397	0.00279	0.00883
Total	0.16929	0.03478	0.26457
Shrouds	0.1157	0.01703	-0.00002
Total w/ shrds	0.28499	0.05181	0.26455

NLS 1 1/2 Stage Airload Distribution Mach 0.95			
Aref=594. ft**2		Dref=330.0 in	
X/D	dCA/d(X/D)	dCNa/d(X/D)	dCMa/d(X/D)
0	0.00204	0.0005	0.00721
0.009	0.14557	0.0005	0.00721
0.021	0.27403	0.00076	0.00966
0.03	0.28976	0.00165	0.01801
0.045	0.1971	0.00535	0.05245
0.051	0.1565	0.0059	0.05754
0.06	0.16157	0.0062	0.06031
0.091	0.17825	0.00745	0.07174
0.103	0.18335	0.00834	0.07995
0.133	0.19318	0.00885	0.08441
0.163	0.19409	0.00976	0.09269
0.194	0.19502	0.01104	0.10425
0.224	0.15222	0.01159	0.10906
0.254	0.06752	0.00981	0.09242
0.27	0.00642	0.00882	0.08327
0.315	-0.01015	0.02514	0.23062
0.37	0.06867	0.01301	0.12005
0.424	0.09706	0.01264	0.11611
0.466	0.10202	0.01326	0.12113
0.576	0.07526	0.01569	0.14125
0.648	0.04858	0.01299	0.11664
0.703	-0.3178	0.00542	0.05002
0.722	-0.66517	0.00389	0.03662
0.76	0.0043	0.00879	0.07829
0.8	0.0043	0.01279	0.11206
0.96	0.0043	-0.00293	-0.02155
1.194	0.0043	-0.02425	-0.19419
1.28	0.0043	-0.01258	-0.09809
1.376	0.0043	-0.00128	-0.00699
1.61	0.0043	-0.00104	-0.00473
1.845	0.0043	-0.0009	-0.00332
2.3	0.0043	0.001	0.01074
2.35	0.0043	0.001	0.01071
2.709	0.0043	0.00394	0.02998
2.921	0.42536	0.01928	0.12937
3.073	0.35017	0.01595	0.10561
3.224	0.29104	0.01833	0.11833
3.376	0.0226	0.05808	0.35812
3.497	-0.51277	0.07001	0.40845
3.539	0.0055	0.01075	0.06658
3.588	0.0055	0.00547	0.03577
3.83	0.0055	0.02264	0.129
4.254	0.0055	-0.02688	-0.13181
4.688	0.0055	0.00054	0.00738
5.506	0.0055	0.00179	0.01214
6.891	0.0055	0.00139	0.00937
8.536	0.0055	0.00269	0.01051
9.332	0.0055	0.00269	0.01051
Total	0.21764	0.03851	0.27179
Shrouds	0.16109	0.01523	-0.00161
Total	0.37873	0.05374	0.27018

NLS 1 1/2 Stage Airloads Distribution Mach 1.05			
Aref=594 ft**2		Dref=330.0 in	
x/d	dCA/d(X/D)	dCNa/d(X/D)	dCMa/d(X/D)
0	0	0	0
0.009	0.0960982	0.0001912	0.00178256
0.021	0.1034227	0.00021817	0.00203135
0.03	0.16406785	0.00136383	0.01268638
0.045	0.17008705	0.00368457	0.03421857
0.051	-0.11914045	0.01156718	0.10735503
0.06	0.48425015	0.00351108	0.03255476
0.091	0.30800045	0.00680442	0.06287961
0.103	0.35487535	0.0078663	0.07259808
0.133	0.2045312	0.0108927	0.10020195
0.163	0.21050955	0.012273	0.11253114
0.194	0.21996775	0.01331547	0.12167673
0.224	0.1807698	0.01232227	0.1122312
0.254	0.240844	0.00810398	0.07356796
0.27	0.087267	0.01111565	0.10073002
0.315	0.03443	0.02803866	0.2528246
0.37	0.106619	0.02364982	0.21194966
0.424	0.146054	0.01734352	0.15449605
0.466	0.146784	0.01767653	0.15672014
0.576	0.142647	0.02001502	0.17525149
0.648	0.076661	0.01504078	0.13061416
0.703	-0.281269	0.00601142	0.05187251
0.722	0	0.00439483	0.03783952
0.76	0	0.0050505	0.04329289
0.8	0	0.0059145	0.05046251
0.96	0	0.00709258	0.05937911
1.194	0	0.006858	0.0558104
1.28	0	0.00416092	0.0335037
1.376	0	0.00167567	0.0133316
1.61	0	-8.5083E-05	-0.00065701
1.845	0	-0.002091	-0.01565532
2.3	0	0.00583167	0.04100828
2.35	0	0.00655125	0.04574083
2.709	0.0206937	0.0089028	0.05896323
2.921	0.3640905	0.02414659	0.15480381
3.073	0.363087	0.01566585	0.09805254
3.224	0.3407445	0.01448126	0.08845155
3.376	0.2943189	0.0176481	0.1051121
3.497	-0.0055368	0.02044088	0.11927254
3.539	0	0.00292655	0.01695353
3.588	0	0.00205225	0.01178815
3.83	0	0.01174828	0.06463901
4.254	0	0.01071109	0.05439092
4.688	0	-0.001785	-0.00828954
5.506	0	0.000595	0.00227647
6.891	0	0.000595	0.0014524
8.536	0	0.000595	0.00047362
9.332	0	0.000595	0
total	0.313272	0.042445	0.285462
shrouds	0.215669	0.013268	-0.003296
total w/ shrds	0.528941	0.055713	0.282166

NLS 1 1/2 Stage Airloads Distribution Mach 1.1			
Aref=594 ft^2		Dref=330 in	
X/D	dCA/d(X/D)	dCNa/d(X/D)	dCMa/d(X/D)
0	0	0	0
0.009	0.105695	0.00012783	0.00119179
0.021	0.113525	0.00012783	0.00119026
0.03	0.184827	0.00067567	0.00628505
0.045	0.189765	0.0019735	0.01832789
0.051	0.194798	0.00215233	0.01997581
0.06	0.663158	-0.00376833	-0.03493999
0.091	0.342057	0.00504883	0.04665627
0.103	0.389134	0.005725	0.05283603
0.133	0.227467	0.00779933	0.07174607
0.163	0.242939	0.008922	0.08180582
0.194	0.251427	0.01002783	0.09163434
0.224	0.197952	0.0145305	0.13234379
0.254	0.211753	0.01812583	0.16454632
0.27	0.052785	0.025371	0.229912
0.315	0.036302	0.03007567	0.27119229
0.37	0.081736	0.0247575	0.22187672
0.424	0.150007	0.015332	0.13657746
0.466	0.170634	0.01133517	0.10049759
0.576	0.173693	0.0129555	0.11343836
0.648	0.111439	0.01141533	0.09913075
0.703	-0.253954	0.004671	0.04030606
0.722	0	0.00393167	0.03385165
0.76	0	0.0042775	0.03666673
0.8	0	0.00521317	0.04447874
0.96	0	0.007065	0.05914818
1.194	0	0.0062895	0.05118395
1.28	0	0.00434033	0.03494836
1.376	0	0.00185175	0.01473252
1.61	0	-0.00017883	-0.00138095
1.845	0	-0.00217442	-0.01627986
2.3	0	0.00381575	0.02683235
2.35	0	0.0059245	0.04136486
2.709	0.024221	0.01118163	0.07405591
2.921	0.416568	0.02824439	0.18107476
3.073	0.432821	0.01961003	0.12273916
3.224	0.414426	0.017461	0.10665179
3.376	0.377428	0.02048681	0.12201946
3.497	0.058268	0.02312794	0.13495153
3.539	0	0.00044454	0.0025752
3.588	0	0.0012941	0.00743329
3.83	0	0.0058357	0.03210804
4.254	0	0.00617729	0.03136828
4.688	0	0.00053346	0.00247739
5.506	0	0.00053346	0.00204102
6.891	0	0.00051997	0.00126925
8.536	0	0.00051997	0.0004139
9.332	0	0.00051997	0
Total	0.378364	0.4043175	0.2716901
Shrouds	0.217327	0.0166	-0.003803
Total	0.595691	0.4209175	0.2678871

NLS 1 1/2 Stage Airload Distribution Mach 1.25			
Aref=594 ft**2		Dref=330 in	
X/D	dCA/d(X/D)	dCNA/d(X/D)	dCMA/(X/D)
0	0	0	0
0.009	0.15244	0	0
0.021	0.29357	0.00012	0.00018
0.03	0.32229	0.00059	0.00454
0.045	0.23661	0.0034	0.03075
0.051	0.19332	0.00441	0.0401
0.06	0.20169	0.00465	0.04234
0.091	0.22541	0.00571	0.05208
0.103	0.23458	0.00588	0.05358
0.133	0.26026	0.00677	0.06166
0.163	0.27801	0.00758	0.06901
0.194	0.28703	0.00829	0.07535
0.224	0.29167	0.00907	0.0823
0.254	0.26518	0.01091	0.09893
0.27	-0.06416	0.01518	0.13786
0.315	0.01797	0.01871	0.16861
0.37	0.08393	0.02208	0.19809
0.424	0.12698	0.02364	0.21091
0.466	0.1471	0.02529	0.22474
0.576	0.17004	0.01986	0.17424
0.648	0.18952	0.01159	0.10044
0.703	0.18016	0.01368	0.11802
0.722	-0.24822	0.00702	0.05994
0.76	0.000245	0.00621	0.05211
0.8	0.000245	0.00735	0.06151
0.96	0.000245	0.00735	0.0603
1.194	0.000245	0.01102	0.08845
1.28	0.000245	0.0073	0.05756
1.376	0.000245	0.0038	0.02898
1.61	0.000245	0.00183	0.0128
1.845	0.000245	0	0
2.3	0.000245	0	0
2.35	0.000245	0	0
2.709	0.000245	-0.0078	-0.05327
2.921	0.33145	0.02899	0.18698
3.073	0.43217	0.03818	0.2415
3.224	0.45032	0.03006	0.18566
3.376	0.44013	0.03042	0.18371
3.497	0.33843	0.03912	0.23239
3.539	0.0002	0.00964	0.05408
3.588	0.0002	0.0102	0.05682
3.83	0.0002	0.017	0.09169
4.254	0.0002	0.00946	0.04609
4.688	0.0002	0.00429	0.01788
5.506	0.0002	-0.00715	-0.02956
6.891	0.0002	0.00072	0.001757
8.536	0.0002	0.0005	0.00095385
9.332	0.0002	1.00E-04	0
TOTAL	0.397424	0.045364	0.311993
Shrouds	0.206716	0.012277	-0.001671
Total w/ shrds	0.60414	0.057641	0.310322

NLS 1 1/2 STAGE AIRLOADS DISTRIBUTION Mach 1.46			
Aref = 594. ft**2		Dref = 330.0 in	
X/D	dCA/d(X/D)	dCNa/d(X/D)	dCMa/d(X/D)
0	0.00193	0.00021	0.00196
0.009	0.13855	0.00021	0.00196
0.021	0.26467	0.00049	0.00456
0.03	0.26875	0.00199	0.01851
0.045	0.15797	0.00764	0.07095
0.051	0.10144	0.01089	0.10107
0.06	0.11132	0.01123	0.10412
0.091	0.13366	0.01239	0.11450
0.103	0.14584	0.01224	0.11296
0.133	0.17134	0.01153	0.10606
0.163	0.20144	0.01064	0.09756
0.194	0.22587	0.01035	0.09458
0.224	0.23543	0.00974	0.08871
0.254	0.23231	0.00862	0.07825
0.27	0.02225	0.00711	0.06443
0.315	0.02977	0.01066	0.09612
0.37	0.0454	0.01198	0.10736
0.424	0.06012	0.01595	0.14208
0.466	0.07472	0.01991	0.17652
0.576	0.0908	0.01727	0.15122
0.648	0.10113	0.01468	0.12748
0.703	0.10444	0.01672	0.14428
0.722	-0.15353	0.0102	0.08782
0.76	0.0043	0.01051	0.09009
0.8	0.0043	0.01015	0.08660
0.96	0.0043	0.00997	0.08347
1.194	0.0043	0.00833	0.06779
1.28	0.0043	0.00558	0.04493
1.376	0.0043	0.00397	0.03159
1.61	0.0043	0.00288	0.02224
1.845	0.0043	0.0019	0.01423
2.3	0.0043	0.00128	0.00900
2.35	0.0043	0.00092	0.00642
2.709	0.0043	-0.01886	-0.12491
2.921	0.20371	0.01558	0.09988
3.073	0.28601	0.0229	0.14333
3.224	0.30771	0.02119	0.12943
3.376	0.33553	0.02764	0.16462
3.497	0.31455	0.03872	0.22593
3.539	0.0055	0.01147	0.06645
3.588	0.0055	0.0116	0.06663
3.83	0.0055	0.01264	0.06955
4.254	0.0055	0.01397	0.07094
4.688	0.0055	0.00875	0.04064
5.506	0.0055	0.00017	0.00065
6.891	0.0055	0.00062	0.00151
8.536	0.0055	0.00109	0.00087
9.332	0.0055	0.00109	0.00000
Total	0.3156	0.04908	0.30779
Shrouds	0.18107	0.00852	-0.00219
Total w/ Shrds	0.49667	0.0576	0.30560

REPORT DOCUMENTATION PAGE

Form Approved
OMB No. 0704-0188

1. AGENCY USE ONLY (Leave blank)	2. REPORT DATE	3. REPORT TYPE AND DATES COVERED
	May 1994	Technical Paper

4. TITLE AND SUBTITLE

Aerodynamic Characteristics of the National Launch System (NLS) 1½ Stage Launch Vehicle

5. FUNDING NUMBERS

6. AUTHOR(S)

A.M. Springer and D.C. Pokora

7. PERFORMING ORGANIZATION NAME(S) AND ADDRESS(ES)

George C. Marshall Space Flight Center
Marshall Space Flight Center, Alabama 35812

8. PERFORMING ORGANIZATION REPORT NUMBER

M-751

9. SPONSORING/MONITORING AGENCY NAME(S) AND ADDRESS(ES)

National Aeronautics and Space Administration
Washington, DC 20546

10. SPONSORING/MONITORING AGENCY REPORT NUMBER

NASA TP-3488

11. SUPPLEMENTARY NOTES

Prepared by the Structures and Dynamics Laboratory, Science and Engineering Directorate.

12a. DISTRIBUTION/AVAILABILITY STATEMENT

Unclassified—Unlimited
Subject Category: 02

12b. DISTRIBUTION CODE

13. ABSTRACT *(Maximum 200 words)*

The National Aeronautics and Space Administration (NASA) is studying ways of assuring more reliable and cost effective means to space. One launch system studied was the NLS which included the 1½ stage vehicle. This document encompasses the aerodynamic characteristics of the 1½ stage vehicle. To support the detailed configuration definition two wind tunnel tests were conducted in the NASA Marshall Space Flight Center's 14×14-Inch Trisonic Wind Tunnel during 1992. The tests were a static stability and a pressure test, each utilizing 0.004 scale models. The static stability test resulted in the forces and moments acting on the vehicle. The aerodynamics for the reference configuration with and without feedlines and an evaluation of three proposed engine shroud configurations were also determined. The pressure test resulted in pressure distributions over the reference vehicle with and without feedlines including the reference engine shrouds. These pressure distributions were integrated and balanced to the static stability coefficients resulting in distributed aerodynamic loads on the vehicle. The wind tunnel tests covered a Mach range of 0.60 to 4.96. These ascent flight aerodynamic characteristics provide the basis for trajectory and performance analysis, loads determination, and guidance and control evaluation.

14. SUBJECT TERMS

National Launch System, 1½ stage, wind tunnel testing, launch vehicle, aerodynamic characteristics, static stability test, pressure test, ascent flight

15. NUMBER OF PAGES

58

16. PRICE CODE

A04

17. SECURITY CLASSIFICATION OF REPORT	18. SECURITY CLASSIFICATION OF THIS PAGE	19. SECURITY CLASSIFICATION OF ABSTRACT	20. LIMITATION OF ABSTRACT
Unclassified	Unclassified	Unclassified	Unlimited

National Aeronautics and
Space Administration
Code JTT
Washington, DC
20546–0001

Official Business
Penalty for Private Use, $300

Postmaster: If Undeliverable (Section 158 Postal Manual), Do Not Return